Published OnlineFirst July 23, 2015; DOI: 10.1158/0008-5472.CAN-15-0405

Microenvironment and Immunology

Cancer Research

Tumor-Promoting Effects of Myeloid-Derived Suppressor Cells Are Potentiated by Hypoxia-Induced Expression of miR-210

Muhammad Zaeem Noman[1], Bassam Janji[2], Shijun Hu[3,4], Joseph C. Wu[3,4], Fabio Martelli[5], Vincenzo Bronte[6], and Salem Chouaib[1]

Abstract

Myeloid-derived suppressor cells (MDSC) contribute significantly to the malignant characters conferred by hypoxic tumor microenvironments. However, selective biomarkers of MDSC function in this critical setting have not been defined. Here, we report that miR-210 expression is elevated by hypoxia-inducible factor-1α (HIF1α) in MDSC localized to tumors, compared with splenic MDSC from tumor-bearing mice. In tumor MDSC, we determined that HIF1α was bound directly to a transcriptionally active hypoxia-response element in the miR-210 proximal promoter. miR-210 overexpression was sufficient to enhance MDSC-mediated T-cell suppression under normoxic conditions, while targeting hypoxia-induced miR-210 was sufficient to decrease MDSC function against T cells. Mechanistic investigations revealed that miR-210 modulated MDSC function by increasing arginase activity and nitric oxide production, without affecting reactive oxygen species, IL6, or IL10 production or expression of PD-L1. In splenic MDSC, miR-210 regulated Arg1, Cxcl12, and IL16 at the levels of both mRNA and protein, the reversal of which under normoxic conditions decreased T-cell–suppressive effects and IFNγ production. Interestingly, miR-210 overexpression or targeting IL16 or CXCL12 enhanced the immunosuppressive activity of MDSC *in vivo*, resulting in increased tumor growth. Taken together, these results provide a preclinical rationale to explore miR-210 inhibitory oligonucleotides as adjuvants to boost immunotherapeutic responses in cancer patients. *Cancer Res; 75(18); 3771–87. ©2015 AACR.*

Introduction

As a common feature of solid tumors, and one of the hallmarks of the tumor microenvironment, hypoxia is currently attracting increased attention in the field of cancer immunology and immunotherapy. The hypoxia-inducible factor (HIF) family of transcription factors are major oxygen sensors and mediate cellular adaptation to hypoxic microenvironment (1, 2).

Several studies have outlined the diverse effects of hypoxia on innate and adaptive immune systems. In general, hypoxia amplifies the activity of innate immune cells while suppressing the response of the adaptive immune system (1, 3). In this regard, it has been reported that hypoxic zones in tumors attract a variety of immune cells, such as myeloid-derived suppressor cells (MDSC), tumor-associated macrophages (TAM), and regulatory T cells (Treg; ref. 1). Tissue-specific targeting of HIF1α in macrophages abrogated their transcriptional response to hypoxia (4). TAM expression of HIF1α was shown to suppress T-cell function and promote tumor progression in a murine model of breast cancer (5). Similarly, hypoxia promoted the recruitment of the immunosuppressive Tregs through the induction of CCL28 expression by hypoxic tumor cells (6). In addition, hypoxia was shown to induce T-cell differentiation into Tregs by promoting HIF1α-dependent induction of FoxP3 (7). Corzo and colleagues (8) have reported that hypoxia via HIF1α altered the function of MDSC in the tumor microenvironment and redirected their differentiation toward TAM.

MDSCs are major players in the orchestration of an immunosuppressive network in many pathologic conditions, such as chronic inflammation and cancer (9). They accumulate in large numbers and undergo dramatic expansion in lymphoid tissues of tumor-bearing hosts. Several studies have extensively described the mechanisms of MDSC-mediated immune suppression (10). However, the relationship between hypoxia-induced microRNA (miRNA; miR) and MDSC function remains unknown.

Accumulating evidence indicates that miRNAs play an important role in regulating immune cell development and in modulating innate and adaptive immune responses (11). In this regard, several miRNAs were reported to regulate macrophage and MDSC differentiation and function. Although miR-155 was induced upon lipopolysaccharide (LPS) stimulation during the macrophage inflammatory responses and shown to target SHIP1 (12), miR-142-3p was identified as essential for preventing macrophage differentiation during tumor-induced myelopoiesis (13). With respect to MDSCs, both miR-17-5p and miR-20a have been

[1]Unité INSERM U1186, Gustave Roussy, Villejuif, France. [2]Laboratory of Experimental Hemato-Oncology, Department of Oncology, Public Research Center for Health (CRP-Santé), Luxembourg City, Luxembourg. [3]Department of Medicine, Division of Cardiology, Stanford, California. [4]Department of Radiology, Molecular Imaging Program, Stanford, California. [5]Molecular Cardiology Laboratory, IRCCS-Policlinico San Donato, San Donato Milanese, Milan, Italy. [6]VeronaUniversity, P. le L.A. Scuro 10, Verona, Italy.

Note: Supplementary data for this article are available at Cancer Research Online (http://cancerres.aacrjournals.org/).

Bassam Janji and Shijun Hu contributed equally to this article.

Corresponding Author: Salem Chouaib, Unité INSERM U1186, Gustave Roussy, 114 rue Edouard Vaillant, 94805 Villejuif, France. Phone: 33-142114547; Fax: 33-142115288; E-mail: chouaib@igr.fr

doi: 10.1158/0008-5472.CAN-15-0405

Published OnlineFirst July 23, 2015; DOI: 10.1158/0008-5472.CAN-15-0405

reported to improve their immunosuppressive potential by modulating STAT3 expression (14). Liu and colleagues (15) have shown that miR-494 was required for the accumulation and functionality of tumor-derived MDSCs. Recently, Wang and colleagues (16) provided data indicating that miR-155 deficiency enhanced MDSCs function and MDSC recruitment in tumor microenvironment.

Hypoxia was shown to regulate the differentiation and function of MDSCs (8). Very recently, we demonstrated that hypoxia via HIF1α selectively upregulated PD-L1 on MDSCs (17). Hypoxia is known to induce a unique subset of miRNAs: hypoxia-induced miRNAs (HIM) in several cell types (18). Hypoxia's influence on HIM in MDSC, as well as their putative contribution on MDSC function, is still unknown. In this study, we demonstrated that hypoxia via HIF1α selectively induced miR-210 in splenic MDSCs, which, in turn, enhanced the MDSC function by increasing Arg-1 expression and by targeting Il16 and Cxcl12.

Materials and Methods

Mice and tumor models

Female C57BL/6 (Charles River) and BALB/c (Harlan) mice were housed at Gustave Roussy animal facility and the experiments were conducted in accordance with EU Directive 63/2010. All experiments with mice were approved by Animal Experimentation and Ethics Committee of the Institut Gustave Roussy (CEEA IRCIV/IGR n° 26, registered at the French Ministry of Research). Seven- to 8-week old mice ($n = 5$ per group) were inoculated subcutaneously (s.c.) with B16-F10 melanoma and 4T1 mammary carcinoma mouse tumor cells, both obtained from the ATCC. Different numbers of tumor cells were inoculated for different models. Tumors were used when they reached at around 1.5 cm in diameter. MDSC immortalized cell line MSC-1 was kindly provided by Prof. Vincenzo Bronte (Verona University, Verona, Italy).

Reagents and antibodies

RPMI-1640, DMEM, FBS, and antibiotics were obtained from Life Technologies. Recombinant murine GM-CSF, anti-ARG-1 FITC, anti-CXCL12 APC, and IL2 were obtained from R&D Systems. The following antibodies were purchased from BioLegend: anti-IL16 PE; from BD Biosciences, anti-iNOS FITC; and from eBioscience, anti-Gr1 FITC, anti-Gr1 PE, anti-Gr1 APC, anti-$Cd11b^+$ PE, anti-$Cd11b^+$ APC, anti-PD-L1 PE, anti-PD-L1 FITC, anti-PD-L1 APC, anti-PD-L2 PE, anti-PD-1 APC, anti-CTLA-4 APC, anti-CD4 FITC, anti-CD8 FITC, anti-IFN-γ APC, anti-CD25 APC, anti-CD25 FTIC, anti-IL6 FITC, anti-IL10 APC, and anti-IL12p70 PE. For blocking, control antibody (IgG; eBioscience: Rat IgG2b K Isotype Control Functional Grade Purified, 16-4031), anti-mouse IL16 Functional Grade Purified neutralizing antibody (BioLegend: 519102), or anti-mouse CXCL12 Functional Grade Purified neutralizing antibody (BD Biosciences: MAB310) were used.

Hypoxic conditioning of MDSCs

MDSCs were cultured in RPMI medium containing 10 ng/mL GM-CSF under hypoxia (0.1% pO_2 with 5% CO_2) in a hypoxia chamber (InVivo2 400 Hypoxia Workstation; Ruskinn).

miR-210 overexpression and knockdown

For miR-210 overexpression, MDSCs were transfected with either Lenti-PremiR-control or Lenti-PremiR-210 (19) under normoxia by using Polybrene (Sigma). miR-210 targeting was performed under hypoxia, and MDSCs were transfected with either anti-miR-control or anti-miR-210 (Life technologies) by using Lipofectamine RNAiMAX Transfection Reagent (Life technologies) according to the manufacturer's instructions.

RNA isolation and SYBR Green qRT-PCR

Total RNA was extracted from the samples with TRIzol solution (Invitrogen). DNase I–treated 1 μg of total RNA was converted into cDNA by using TaqMan Reverse transcription reagent (Applied Biosystems) and mRNAs levels were quantified by the SYBR Green qPCR method (Applied Biosystems). Relative expression was calculated by using the comparative C_T method ($-2^{\Delta C_T}$).

miRNA (isolation and detection)

For extraction of miRNAs, TRIzol (Invitrogen) was used. DNase I–treated total RNA (8 ng) was subjected to quantitative RT-PCR (qRT-PCR) analysis using the TaqMan miR Reverse Transcription Kit (Applied Biosystems). Different miRNAs levels were quantified by using miRNA-specific TaqMan primers from Life Technologies. Expression levels of mature miRNAs were evaluated using the comparative C_T method ($-2\Delta C_T$). Transcript levels of U6 were used as an endogenous control.

Western blot analysis

Western blot analysis was performed as previously reported (17).

Flow cytometry analysis

Flow cytometry was performed using FACS LSR-II. Data were further analyzed by FACS DIVA 7.0 or Flow Jo 7.6.5 software.

Gene silencing by RNA interference

Predesigned siRNA against HIF1α, HIF2α, Arg-1, Ndrg1, and scrambled control were obtained from Life Technologies and transfected by electroporation as described earlier (17).

MDSC isolation from spleens and tumors of tumor-bearing mice

Single-cell suspensions were prepared from spleens by mechanical dissociation, followed by removal of red blood cells with ammonium chloride lysis buffer (ACK). Solid tumors were dissected and mechanically dissociated into small, <4-mm fragments with a scalpel, followed by digestion with a mouse tumor dissociation kit (Miltenyi Biotec) for 45 minutes at 37°C. After single-cell suspensions were obtained, red blood cells were removed by ACK and dead cells were depleted with a dead cell removal kit (Miltenyi Biotec). $Gr1^+$ cells were isolated by using either biotinylated or anti-Gr1-APC antibody, and corresponding streptavidin, or anti-APC microbeads on MACS LS columns, according to the manufacturer's protocol (Miltenyi Biotec). This process yielded $Gr1^+$ cells with purity >95% as evaluated by FACS analysis. For RNA isolation, MDSCs were isolated by cell sorting on FACS MOFlo or FACSAria (BD) after incubating with APC-conjugated anti–Gr-1 antibody and FITC-conjugated anti-CD11b antibodies.

Published OnlineFirst July 23, 2015; DOI: 10.1158/0008-5472.CAN-15-0405

miR-210 detection by the Flow-FISH method using flow cytometry

MDSCs ($Gr1^+$ cells) from splenic and tumor single-cell suspensions were stained with viability dye (Invitrogen LIVE/DEAD UV), anti-Gr1 FITC and anti-$Cd11b^+$ PE for 30 minutes on ice. The Flow-FISH assay for miR-210 was performed as per the manufacturer's instructions (Affymetrix, Inc.). Briefly, MDSCs were fixed with a 4% paraformaldehyde solution for 1 hour at room temperature. Cells were then permeabilized with ice-cold methanol, followed by further fixation with a 4% paraformaldehyde solution for 30 minutes at room temperature. All buffers used in the following steps were included in the manufacturer's kit. To detect mRNA, probes composed of 20 oligonucleotide base pairs against the mRNA of interest were used. Currently, there are three different types of probes with unique tag sequences, named type 1, type 4, and type 6, respectively. Each tag sequence allows the hybridization of specific complementary branched DNA nanostructure with different excitation/emission spectra: type 1–650/668, type 4–495/519, and type 6–749/775. miR-210 and irrelevant probes were diluted 1:20 in target probe diluent, added to the cell suspension and allowed to hybridize to the target RNA for 2 hours at 40°C. Excess probe was removed by adding wash buffer followed by centrifugation at 800 × *g* for 5 minutes. Signal amplification was achieved by performing sequential hybridization with DNA branches (i.e., Pre-Amplifier and Amplifier). The first DNA branch in the PreAmp Mix was added at a 1:1 ratio and was allowed to hybridize for 1.5 hours at 40°C. Samples were washed with wash buffer, and then the second DNA branch in the Amp Mix was added at a 1:1 ratio and hybridized for 1.5 hours at 40°C. Samples were washed with wash buffer before addition of the label probes. For signal detection, fluorochrome-conjugated label probes (Alexa Fluor 647) were diluted 1:100 in label probe diluent, added to the samples and allowed to hybridize for 1 hour at 40°C. Finally, MDSCs were washed with wash buffer, transferred to the storage buffer and subsequently analyzed on a LSR Fortessa, using FACS DIVA software version 8 (BD Biosciences). Flow cytometric data were analyzed with FlowJo Version 10 (TreeStar). As negative controls, irrelevant probe was used.

MDSCs functional assays

For evaluation of T-cell proliferation, splenocytes from B16-F10 or 4T1 tumor-bearing mice were plated into U-bottom 96-well plates along with MDSCs at different ratios (50,000 MDSC: 200,000 splenocytes per well). Plates were stimulated with anti-CD3/CD28 beads (Miltenyi Biotec) for 72 hours at 37°C. Cocultures were pulsed with thymidine (1 μCi/well; Promega) for 16 to 18 hours before harvesting. ^{3}H-thymidine uptake was counted using Packard's TopCountNXT liquid scintillation counter and expressed as counts per minute (CPM). For assessment of T-cell functions, MDSCs, cocultured with splenocytes from B16-F10 or 4T1 tumor-bearing mice, were stimulated with anti-CD3/CD28 beads. After 72 hours, intracellular IFNγ production was evaluated by flow cytometry by gating on $CD3^+CD8^+$ $IFN\gamma^+$ and $CD3^+CD4^+$ $IFN\gamma^+$ populations.

MDSCs cytokine production

MDSC isolated from spleens of B16-F10 and 4T1 tumor-bearing mice were cultured under normoxia and hypoxia for 72 hours. Supernatants were collected and the secretion of IL6, IL10, IL16, and CXCL12 (eBioscience) was determined by ELISA.

Arginase enzymatic activity and nitric oxide production

Arginase activity was measured in MDSC cell lysates as described previously (8). For nitric oxide (NO) production, culture supernatants were mixed with Greiss reagent and nitrite concentrations were determined as described earlier (8).

Reactive oxygen species detection

Reactive oxygen species (ROS) production was measured by using oxidation-sensitive dye DCFDA (Invitrogen; ref. 8). Briefly, MDSC isolated from spleens of B16-F10 and 4T1 tumor-bearing mice were cultured under normoxia and hypoxia for 72 hours followed by incubation at 37°C in RPMI in the presence of 2.5 μmol/L DCFDA for 30 minutes.

Chromatin immunoprecipitation assay

Chromatin immunoprecipitation (ChIP) was performed with lysates prepared from MSC-1 by using the SimpleChIP Enzymatic Chromatin IP Kit (Cell Signaling Technology). SYBR Green RT-qPCR was performed using the primers detailed in Supplementary Table S2.

Luciferase reporter assay for HRE in miR-210 promoter

A 565-bp fragment corresponding to mouse miR-210 promoter containing HRE-1/2 sequence was inserted into the *Bgl*II and *Hin*dIII sites of pGL2-Basic vector (Promega). The hypoxia response elements (HRE; A/GCGTG) were mutated to A/GAAAG and different HRE-1/2 mutants were generated as described previously (20). MSC-1 cells were cotransfected with 0.2 μg of pGL4-hRluc/SV40 (which contains *Renilla* luciferase sequences downstream of the SV40 promoter) vector and 1ug of pGL2 HRE-1/2, pGL2 HRE-1/2 MUT-1, pGL2 HRE-1/2 MUT-2, and pGL2 HRE-1/2 MUT-1+2 vectors in 6-well plates with Lipofectamine 2000 (Invitrogen) in OPTIMEM (Invitrogen) medium and grown under normoxia or hypoxia. After 48 hours, firefly and *Renilla* luciferase activities were measured using the Dual-Luciferase Reporter assay (Promega) and the ratio of firefly:*Renilla* Luciferase was determined.

Luciferase reporter assay for miR-210 target gene validation

mmu-miR-210–binding sites sequence from the 3′-untranslated region (UTR), 5′-UTR, or CDS of Arg1,Cxcl12, Il16, and Ndrg1 genes were cloned into pSI-check2 vector by PCR amplification of genomic DNA. Primer sequences are available upon request. MSC-1 cells were cotransfected with 800 ng pSI-check-2 and 10 nmol/L of Lenti-PremiR-CT, or Lenti-PremiR-210, in 24-well plates with Lipofectamine 2000 (Invitrogen) in OPTIMEM (Invitrogen) medium. After 48 hours, firefly and *Renilla* luciferase activities were measured using the Dual-Luciferase Reporter assay (Promega) and the ratio of firefly:*Renilla* Luciferase was determined.

Statistical analysis

Data were analyzed with GraphPad Prism. The Student *t* test was used for single comparisons.

Published OnlineFirst July 23, 2015; DOI: 10.1158/0008-5472.CAN-15-0405

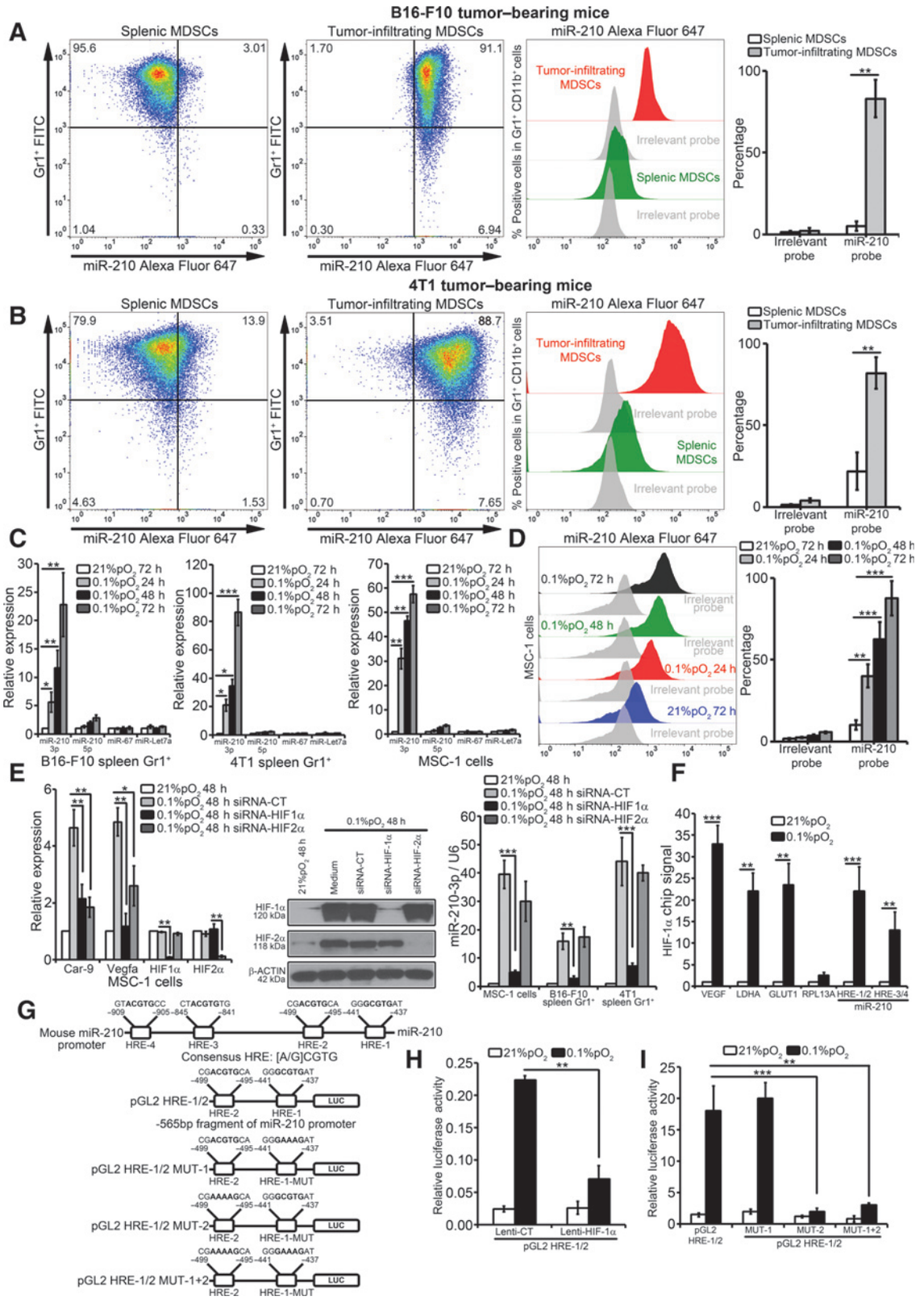

Published OnlineFirst July 23, 2015; DOI: 10.1158/0008-5472.CAN-15-0405

Results

Differential expression of miR-210 on tumor-infiltrating MDSCs versus splenic MDSCs and selective induction of miR-210 via HIF1α in splenic MDSCs under hypoxia

We first compared miR-210 expression between splenic MDSCs and tumor-infiltrating MDSCs from tumor-bearing mice. For this purpose, we used a recently described (21) and cutting-edge technique (Flow-FISH) for miR-210 detection along with anti-$Gr1^+$ and anti-$CD11b^+$ antibodies by flow cytometry directly on splenic and tumor-infiltrating MDSCs. We found that the percentage of miR-210–expressing positive cells was significantly higher on tumor-infiltrating MDSCs as compared with splenic MDSC in both B16-F10 (Fig. 1A) and 4T1 (Fig. 1B) tumor models. No difference was found in MDSCs hybridized with irrelevant probe in splenic MDSCs as compared with tumor-infiltrating MDSCs in two tumor models tested (Fig. 1A and 1B). Interestingly, tumor-infiltrating MDSCs also expressed higher levels of CA-IX and GLUT-1 (2 well-known hypoxia markers) as compared with splenic MDSC in both B16-F10 (Supplementary Fig. S1A) and 4T1 (Supplementary Fig. S1B) tumor models. The higher expression of hypoxia markers undoubtedly demonstrate that tumor-infiltrating MDSCs are found in hypoxic zones.

In order to identify miRNAs that are induced by hypoxia in MDSCs, we selected several HIM's and compared their expression in splenic MDSCs from various tumor-bearing mice, under normoxia or hypoxia, for 24, 48, and 72 hours. We found that hypoxic response genes, such as Ldha, Car-9, Vegfa, and Glut-1, were highly expressed under hypoxia as compared with normoxia in splenic $Gr1^+$ cells from B16-F10 and 4T1 (Supplementary Fig. S1D) tumor-bearing mice. As depicted in Fig. 1C, among the putative HIM's, miR-210 (especially mmu-miR-210-3p) was highly and significantly induced under hypoxia in splenic $Gr1^+$ cells from B16-F10 (more than 30-fold change) and 4T1(more than 100-fold change) tumor-bearing mice. No difference was found in the expression levels of several other miRNAs known to be induced under hypoxia (Fig. 1C and data not shown). Although several miRNAs have been reported to regulate MDSCs function and differentiation (15, 22, 23), it should be noted that we did not observe any difference under hypoxia in the expression levels of miR-21, miR-155, miR-494, and miR-223 in both B16-F10 spleen $Gr1^+$ (Supplementary Fig. S1E) and 4T1 spleen $Gr1^+$ (Supplementary Fig. S1F) cells.

We further investigated whether HIFs, HIF1α or HIF2α, are involved in the induction of miR-210 under hypoxia. For this purpose, we used an already established MDSC cell line, MSC-1 (24), as it is difficult to maintain *ex vivo* MDSC in culture because of their rapid and spontaneous death. We first validated that hypoxia induced miR-210 (more than 60-fold change; Fig. 1C and 1D) and also highly increased the expression levels of various hypoxic response genes such as Ldha, Car-9, Vegfa, and Glut-1 in MSC-1 cells (Supplementary Fig. S1C and S1D). To dissect the roles of HIF1α and HIF2α in miR-210 induction, the MSC-1 cell line was transfected with siRNA targeting HIF1α, HIF2α, or scrambled control (Fig. 1E). The siRNA-mediated knockdown of HIF1α, but not HIF2α, under hypoxia significantly decreased hypoxia-induced miR-210 in MSC-1 cells as well in B16-F10 spleen $Gr1^+$ and 4T1 spleen $Gr1^+$ cells (Fig. 1E).

To investigate whether miR-210 is a direct HIF1α target gene, we searched for potential HIF1α-binding sites in the proximal promoter of mouse mature miR-210 gene using fuzznuc (EMBOSS explorer) software. As shown in Fig. 1G, we found four putative HREs containing the consensus sequence (A/G) CGTG within the mouse mature miR-210 gene.

Using ChIP, we demonstrated hypoxia-inducible binding of HIF1α at four different HRE sites in hypoxic MSC-1 cells (Fig. 1F). ChIP complexes in hypoxic MSC-1 cells showed a significant binding of HIF1α at HRE-1/2 and HRE-3/4 (more than 20-fold for HRE-1/2), comparable with their binding to an established HRE in VEGF, LDHA, and GLUT-1 genes. Moreover, as shown in Fig. 1H, the luciferase activity of HRE-1/2 decreased (more than

Figure 1.

Tumor-infiltrating MDSCs differentially express miR-210 as compared with splenic MDSCs and hypoxia selectively induced miR-210 via HIF1α in splenic MDSCs from tumor-bearing mice. miRNA (mmu-miR-210) was detected by flow cytometry in $Gr1^+$ $CD11b^+$ cells (MDSCs) from B16-F10 (A) and 4T1 (B) in spleens (green histogram) and tumor (red histogram) as compared with control irrelevant probe (gray-shaded histogram). Statistically significant differences (indicated by asterisks) between tumor-infiltrating MDSCs and splenic MDSCs are shown (*, $P < 0.05$; **, $P < 0.005$; ***, $P < 0.0005$). Each tumor model included $n = 3$ mice. Three experiments with the same results were performed. Error bars, SD. C, TaqMan RT-qPCR was used to evaluate different miRNA's expression in B16-F10 spleen $Gr1^+$, 4T1 spleen $Gr1^+$, and MSC-1 cells with or without exposure to 0.1% pO_2 hypoxia at indicated times. Expression levels of U6 were used as endogenous control. D, flow cytometry was used to detect miR-210 expression in MSC-1 cells at indicated conditions. Shown are statistically significant differences (indicated by asterisks) between cells (MSC-1 or spleen $Gr1^+$) cultured under normoxia or hypoxia (*, $P < 0.05$; **, $P < 0.005$; ***, $P < 0.0005$). Three separate experiments (in triplicates) with the same results were performed. Error bars, SD. E, MSC-1 cells were transfected with different siRNA targeting HIF1α, HIF2α, or scrambled control (CT) and cultured under hypoxia for 48 hours. Expression levels of Ldha, Vegfa, HIF1α, and HIF2α were evaluated by SYBR Green RT-qPCR. Western blot analysis was performed to show HIF1α and HIF2α protein levels. β-Actin was used as a control. TaqMan RT-qPCR was used to evaluate miR-210-3p expression levels in MSC-1, B16-F10 spleen $Gr1^+$, and 4T1 spleen $Gr1^+$ cells at indicated conditions. Expression levels of U6 were used as endogenous control. Shown are statistically significant differences (indicated by asterisks) between cells (MSC-1 or spleen $Gr1^+$) transfected with either siRNA-CT and siRNA-HIF1α (*, $P < 0.05$; **, $P < 0.005$; ***, $P < 0.0005$). The experiment was repeated three times with the same results. Error bars, SD. F–I, HIF1α binds directly to the HRE in the miR-210 proximal promoter and induces its expression under hypoxia. F, MSC-1 cells were cultured at normoxia or hypoxia (0.1% pO_2) and ChIP was performed using anti-HIF1α antibody followed by SYBR Green RT-qPCR using Vegfa, Ldha, Glut1, miR-210 HRE sites (HRE-1/2 and HRE-3/4), and RPL13A primers. For each gene, the RT-qPCR signals were normalized to the normoxic condition. Statistically significant differences (indicated by asterisks) between normoxic and hypoxic conditions are shown (*, $P < 0.05$; **, $P < 0.005$). Two separate experiments (in triplicates) with the same results were performed. Error bars, SD. G, different HREs in mouse miR-210 promoter are shown. H, MSC-1 cells transduced with Lenti-CT (control) or Lenti-HIF1α were further cotransfected with pGL4-hRluc/SV40 vector and pGL2 HRE-1/2 vectors and grown under normoxia or hypoxia. After 48 hours, firefly and *Renilla* luciferase activities were measured using the Dual-Luciferase Reporter Assay (Promega) and the ratio of firefly: *Renilla* luciferase was determined. I, MSC-1 cells were cotransfected with pGL4-hRluc/SV40 vector and pGL2 HRE-1/2, pGL2 HRE-1/2 MUT-1, pGL2 HRE-1/2 MUT-2, and pGL2 HRE-1/2 MUT-1+2 vectors and grown under normoxia or hypoxia. After 48 hours, firefly and *Renilla* luciferase activities were measured using the Dual-Luciferase Reporter Assay (Promega) and the ratio of firefly:*Renilla* luciferase was determined. Statistically significant differences (indicated by asterisks) between normoxic and hypoxic conditions are shown (**, $P < 0.005$; ***, $P < 0.0005$). The experiment was performed in triplicates and repeated three times with the same results. Error bars, SD.

Published OnlineFirst July 23, 2015; DOI: 10.1158/0008-5472.CAN-15-0405

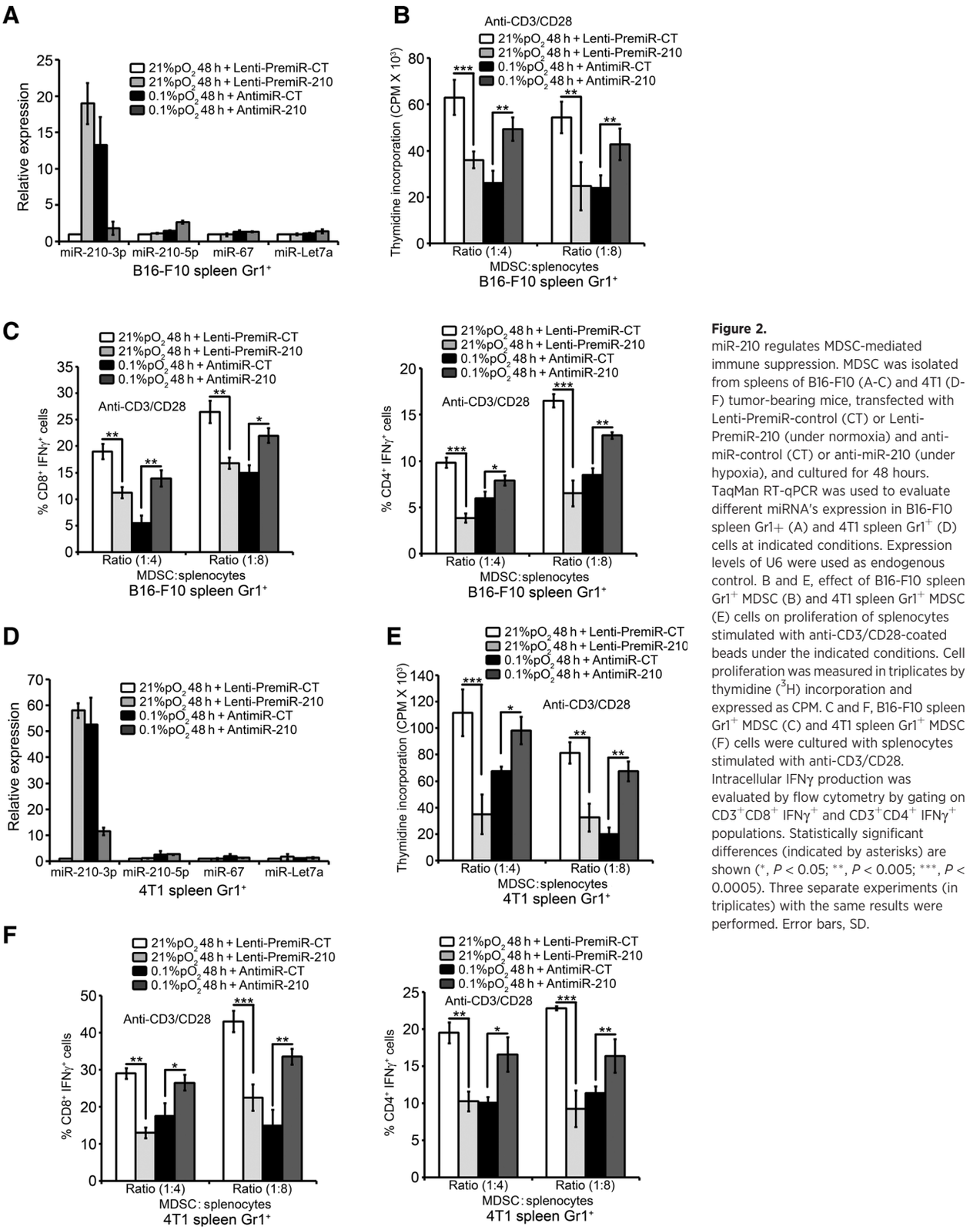

Figure 2.
miR-210 regulates MDSC-mediated immune suppression. MDSC was isolated from spleens of B16-F10 (A-C) and 4T1 (D-F) tumor-bearing mice, transfected with Lenti-PremiR-control (CT) or Lenti-PremiR-210 (under normoxia) and anti-miR-control (CT) or anti-miR-210 (under hypoxia), and cultured for 48 hours. TaqMan RT-qPCR was used to evaluate different miRNA's expression in B16-F10 spleen Gr1+ (A) and 4T1 spleen $Gr1^+$ (D) cells at indicated conditions. Expression levels of U6 were used as endogenous control. B and E, effect of B16-F10 spleen $Gr1^+$ MDSC (B) and 4T1 spleen $Gr1^+$ MDSC (E) cells on proliferation of splenocytes stimulated with anti-CD3/CD28-coated beads under the indicated conditions. Cell proliferation was measured in triplicates by thymidine (^3H) incorporation and expressed as CPM. C and F, B16-F10 spleen $Gr1^+$ MDSC (C) and 4T1 spleen $Gr1^+$ MDSC (F) cells were cultured with splenocytes stimulated with anti-CD3/CD28. Intracellular IFNγ production was evaluated by flow cytometry by gating on $CD3^+CD8^+$ $IFN\gamma^+$ and $CD3^+CD4^+$ $IFN\gamma^+$ populations. Statistically significant differences (indicated by asterisks) are shown (*, $P < 0.05$; **, $P < 0.005$; ***, $P < 0.0005$). Three separate experiments (in triplicates) with the same results were performed. Error bars, SD.

Published OnlineFirst July 23, 2015; DOI: 10.1158/0008-5472.CAN-15-0405

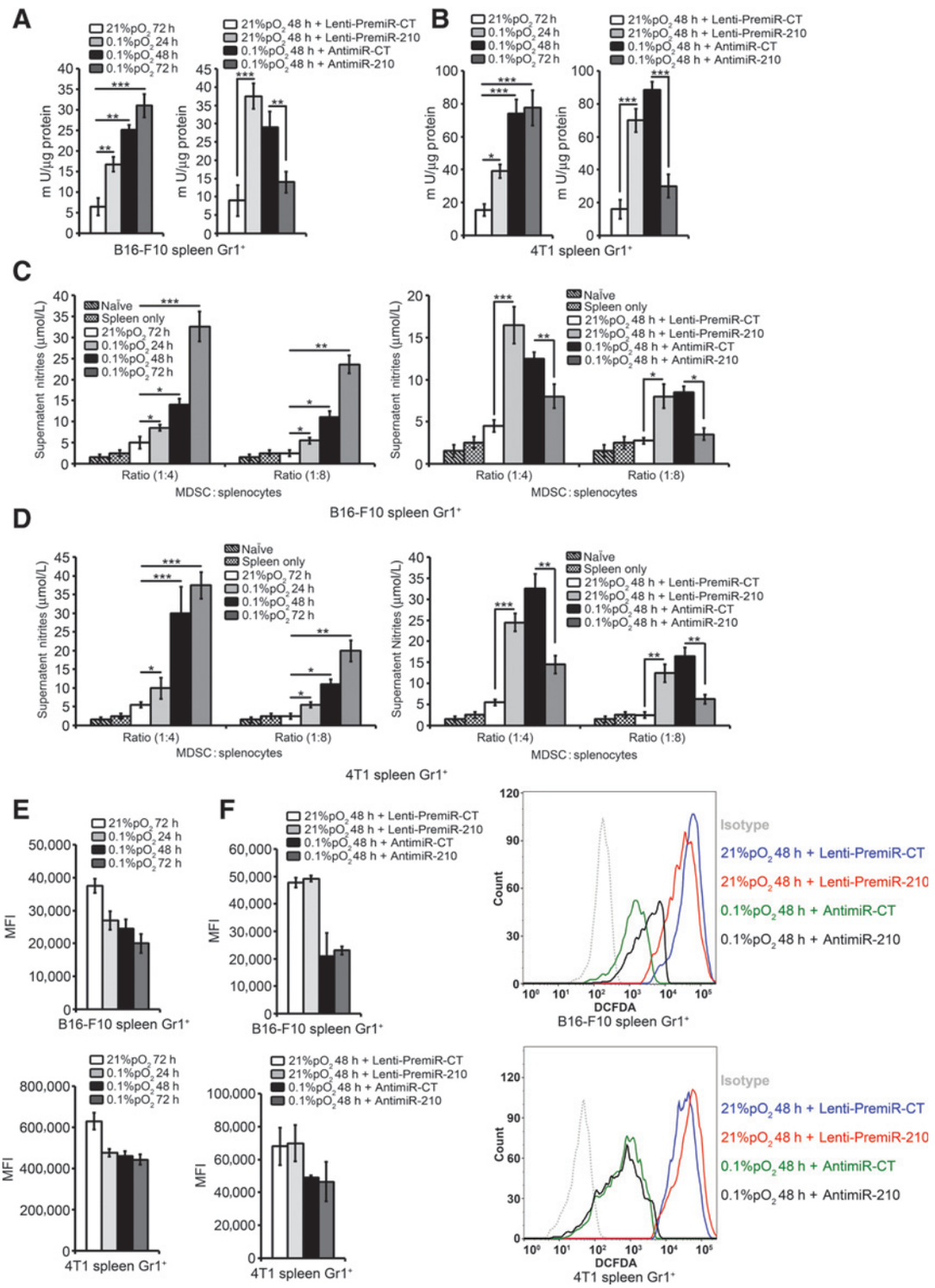

Figure 3.

miR-210 in MDSC regulated their arginase activity and NO production but had no effect on ROS production. MDSC isolated from spleens of B16-F10 and 4T1 tumor-bearing mice, transfected with Lenti-PremiR-control (CT) or Lenti-PremiR-210 (under normoxia) and anti-miR-control (CT) or anti-miR-210 (under hypoxia), was cultured with or without exposure to 0.1% pO_2 hypoxia at indicated times. A and B, arginase enzymatic activity was measured in B16-F10 spleen $Gr1^+$ MDSC (A) and 4T1 spleen $Gr1^+$ MDSC (B) cells under indicated conditions. C and D, after 72 hours of B16-F10 spleen $Gr1^+$ MDSC (C) and 4T1 spleen $Gr1^+$ MDSC (D) cells coculture with splenocytes, supernatants were collected and assayed for nitrites (NO production) under indicated conditions. Statistically significant differences (indicated by asterisks) are shown (*, $P < 0.05$; **, $P < 0.005$; ***, $P < 0.0005$). The experiment was performed in triplicates and repeated three times with the same results. Error bars, SD. E and F, ROS level was evaluated in B16-F10 spleen $Gr1^+$ MDSC (E) and 4T1 spleen $Gr1^+$ MDSC (F) cells by staining with DCFDA at indicated conditions. Isotype control is gray-dotted line in histogram. The experiment was repeated three times with the same results. MFI, mean fluorescence intensity. Error bars, SD.

Published OnlineFirst July 23, 2015; DOI: 10.1158/0008-5472.CAN-15-0405

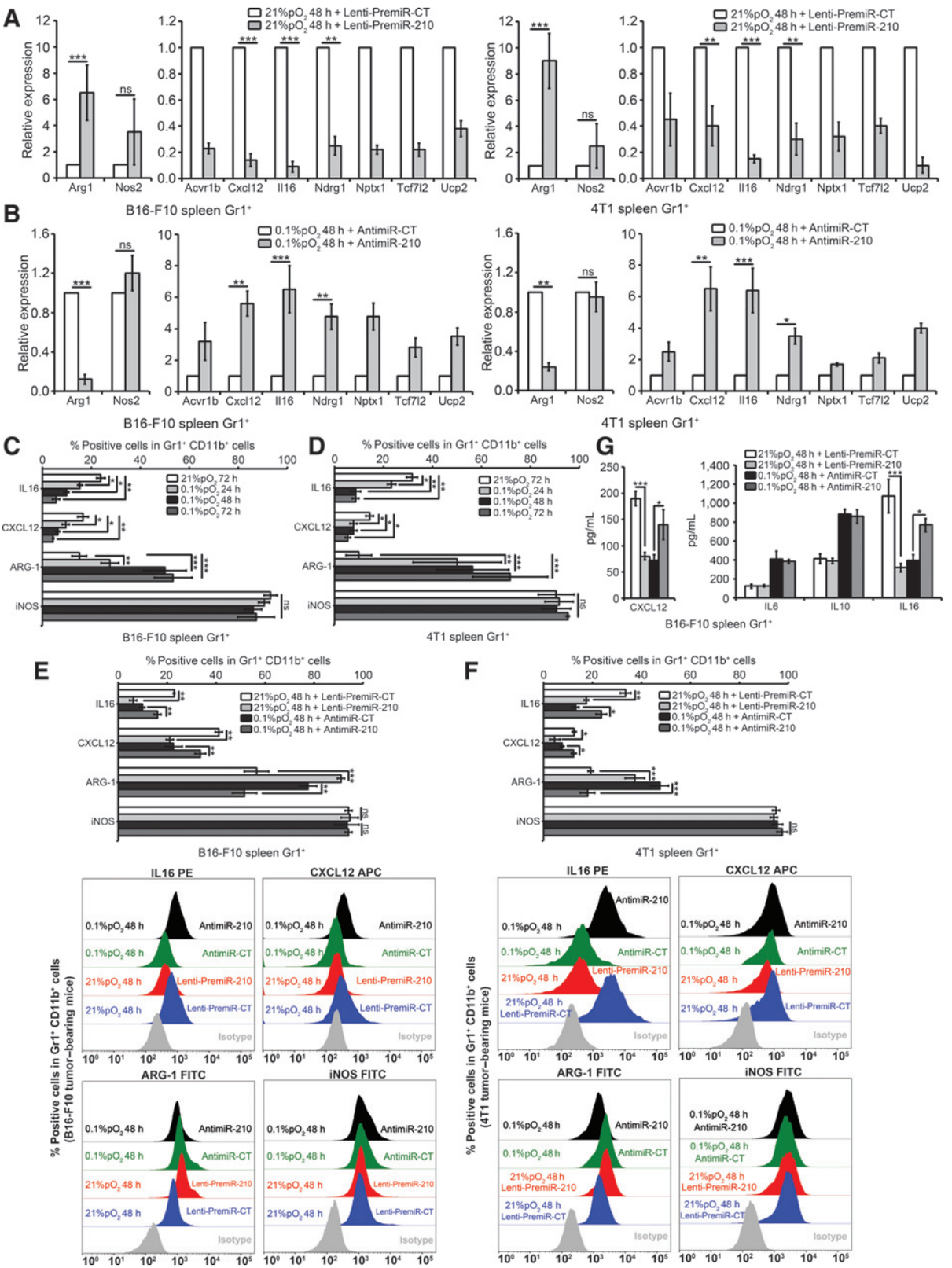

Published OnlineFirst July 23, 2015; DOI: 10.1158/0008-5472.CAN-15-0405

60%) when MSC-1 cells were transduced with Lenti-HIF1α as compared with Lenti-CT.

To determine whether this HIF1α site (HRE-1/2) was a transcriptionally active HRE, MSC-1 cells were cotransfected with pGL4-hRluc/SV40 vector and pGL2 HRE-1/2, pGL2 HRE-1/2 MUT-1, pGL2 HRE-1/2 MUT-2, and pGL2 HRE-1/2 MUT-1+2 vectors (Fig. 1G) and grown under normoxia or hypoxia. After 48 hours, firefly and *Renilla* luciferase activities were measured. As shown in Fig. 1I, hypoxia significantly increased the luciferase activity of HRE-1/2 reporter by more than 15 folds as compared with normoxia. More interestingly, the luciferase activities of HRE-1/2-MUT-2 and HRE-1/2-MUT-1+2 significantly decreased (more than 80%) as compared with HRE-1/2 under hypoxia. The results presented in Figs. 1E–I demonstrate that miR-210 is a direct HIF1α target gene in MSC-1 cells.

These data clearly indicate that tumor-infiltrating MDSCs express increased levels of miR-210 and hypoxia markers (CA-IX and GLUT-1) as compared with splenic MDSCs. We provide evidence here that hypoxia selectively induced miR-210 via HIF1α in splenic MDSCs from tumor-bearing mice.

miR-210 is involved in the regulation of MDSC function

To directly investigate the functional consequences of hypoxia-induced miR-210 in MDSC-mediated T-cell suppression, splenic MDSCs were transfected with Lenti-PremiR-control (CT) or Lenti-PremiR-210 (under normoxia), and anti-miR-control (CT) or anti-miR-210 (under hypoxia), and cultured for 48 hours. Transfection with Lenti-PremiR-210 resulted in the overexpression of miR-210 under normoxia in B16-F10 spleen $Gr1^+$ (25-fold as compared with 30-fold under hypoxia) and 4T1 spleen $Gr1^+$ (60-fold as compared with 100-fold under hypoxia) cells (Fig. 2A and 2D). A transfection with anti-miR-210 resulted in the abrogation of miR-210 expression under hypoxia in B16-F10 spleen $Gr1^+$ (Fig. 2A) and 4T1 spleen $Gr1^+$ (Fig. 2D) cells.

As shown in Fig. 2B and E, hypoxia significantly increased the ability of splenic MDSCs (from B16-F10 and 4T1 tumor-bearing mice) to suppress nonspecific stimuli (anti-CD3/CD28 antibody)–mediated T-cell proliferation. Interestingly, overexpression of miR-210 under normoxia significantly increased the suppressive activity of both B16-F10 splenic MDSCs (Fig. 2B) and 4T1 splenic MDSCs (Fig. 2E) in response to nonspecific stimuli (anti-CD3/CD28 antibody). On the contrary, targeting miR-210 under hypoxia significantly abrogated the suppressive activity of both B16-F10 splenic MDSCs (Fig. 2B) and 4T1 splenic MDSCs (Fig. 2E) in response to the same stimuli.

As illustrated in Fig. 2C and F, under hypoxia, splenic MDSCs (from B16-F10 and 4T1 tumor-bearing mice) acquired the increased ability to inhibit T-cell function by decreasing the percentage of $IFN\gamma^+$ cells in $CD8^+$ and $CD4^+$ T-cell populations.

Overexpression of miR-210 under normoxia significantly increased the suppressive activity of both B16-F10 splenic MDSCs (Fig. 2C) and 4T1 splenic MDSCs (Fig. 2F) as the percentage of $IFN\gamma^+$ $CD8^+$ and $IFN\gamma^+$ $CD4^+$ T cells significantly decreased. On the other hand, the percentage of $IFN\gamma^+$ $CD8^+$ and $IFN\gamma^+$ $CD4^+$ T cells increased after miR-210 knockdown in both B16-F10 splenic MDSCs (Fig. 2C) and 4T1 splenic MDSCs (Fig. 2F) under hypoxic conditions. Thus, the overexpression of miR-210 enhanced MDSC-mediated T-cell suppression under normoxia while targeting of hypoxic miR-210 decreased MDSC function. These data strongly indicated that hypoxia-induced miR-210 is involved in mediating the suppressive action of MDSCs.

Hypoxia-induced miR-210 regulates MDSC function by selectively increasing arginase activity and NO production

To determine the underlying mechanism involved in the regulation of MDSCs immunosuppressive activity by hypoxia-induced miR-210, we examined the effects of miR-210 (overexpression and targeting) on MDSC function with regard to their arginase activity, NO, and ROS production. As shown previously by our group (17) and Corzo and colleagues (8), we observed significantly higher levels of arginase activity in splenic MDSCs from B16-F10 (Fig. 3A) and 4T1 (Fig. 3B) under hypoxia. Overexpression of miR-210 under normoxia significantly increased the arginase activity of both B16-F10 splenic MDSCs (Fig. 3A) and 4T1 splenic MDSCs (Fig. 3B); whereas, the arginase activity decreased after miR-210 knockdown in both B16-F10 splenic MDSCs (Fig. 3A) and 4T1 splenic MDSCs (Fig. 3B) under hypoxic conditions. Similarly, splenic MDSCs from B16-F10 (Fig. 3C) and 4T1 (Fig. 3D) had higher levels of NO production under hypoxia. Overexpression of miR-210 under normoxia increased the MDSCs NO production, whereas targeting miR-210 abrogated NO production in both B16-F10 splenic MDSCs (Fig. 3C) and 4T1 splenic MDSCs (Fig. 3D) under hypoxic conditions. Although splenic MDSCs from both B16-F10 (Fig. 3E) and 4T1 (Fig. 3F) displayed significantly lower levels of ROS under hypoxia, we did not detect any effect of miR-210 overexpression (under normoxia) or knockdown (under hypoxia) in these MDSCs (Fig. 3E and F).

We next evaluated the effect of miR-210 on immune checkpoint regulators (PD-L1, PD-L2, PD1, and CTLA-4) as well as the production and secretion of several cytokines by MDSCs. There was no observed effect of miR-210 on either cytokines (Il6, Il10, Il12p70, and Tgfb1; Supplementary Fig. S2A) or immune checkpoint (Pdl1, Pdl2, Pd1, and Ctla-4; Supplementary Fig. S2C) mRNA levels in B16-F10 MDSCs. Similarly, no effect was seen of miR-210 overexpression (under normoxia) or knockdown

Figure 4.

Identification of candidate target genes from a panel of predicted mmu-miR-210 transcripts in splenic MDSCs from tumor-bearing mice. MDSC isolated from spleens of B16-F10 and 4T1 tumor-bearing mice, transfected with Lenti-PremiR-control (CT) or Lenti-PremiR-210 (under normoxia), and anti-miR-control (CT) or anti-miR-210 (under hypoxia) was cultured with or without exposure to 0.1% pO_2 hypoxia at indicated times. A and B, SYBR Green RT-qPCR was used to monitor Arg1, Nos2, Acvr1b, Cxcl12, Il16, Ndrg1, Nptx1, Tcf7l2, and Ucp2 expressions levels at indicated conditions in B16-F10 spleen $Gr1^+$ and 4T1 spleen $Gr1^+$ cells. Expression level of 18S was used as endogenous control. Statistically significant differences (indicated by asterisks) are shown (*, $P < 0.05$; **, $P < 0.005$; ***, $P < 0.0005$). The experiment was performed in triplicates and repeated three times with the same results. Error bars, SD. C–F, intracellular IL16, CXCL12, ARG1, and iNOS were detected by intra-cytoplasmic staining FACS at indicated conditions in B16-F10 spleen $Gr1^+$ (C and E) and 4T1 spleen $Gr1^+$ (D and F) cells. IL6, IL10, IL16, and CXCL12 cytokine secretion by B16-F10 spleen $Gr1^+$ (G) cells was detected by ELISA at indicated conditions. Statistically significant differences (indicated by asterisks) are shown (*, $P < 0.05$; **, $P < 0.005$; ***, $P < 0.0005$). The experiment was repeated three times with the same results. Error bars, SD.

Published OnlineFirst July 23, 2015; DOI: 10.1158/0008-5472.CAN-15-0405

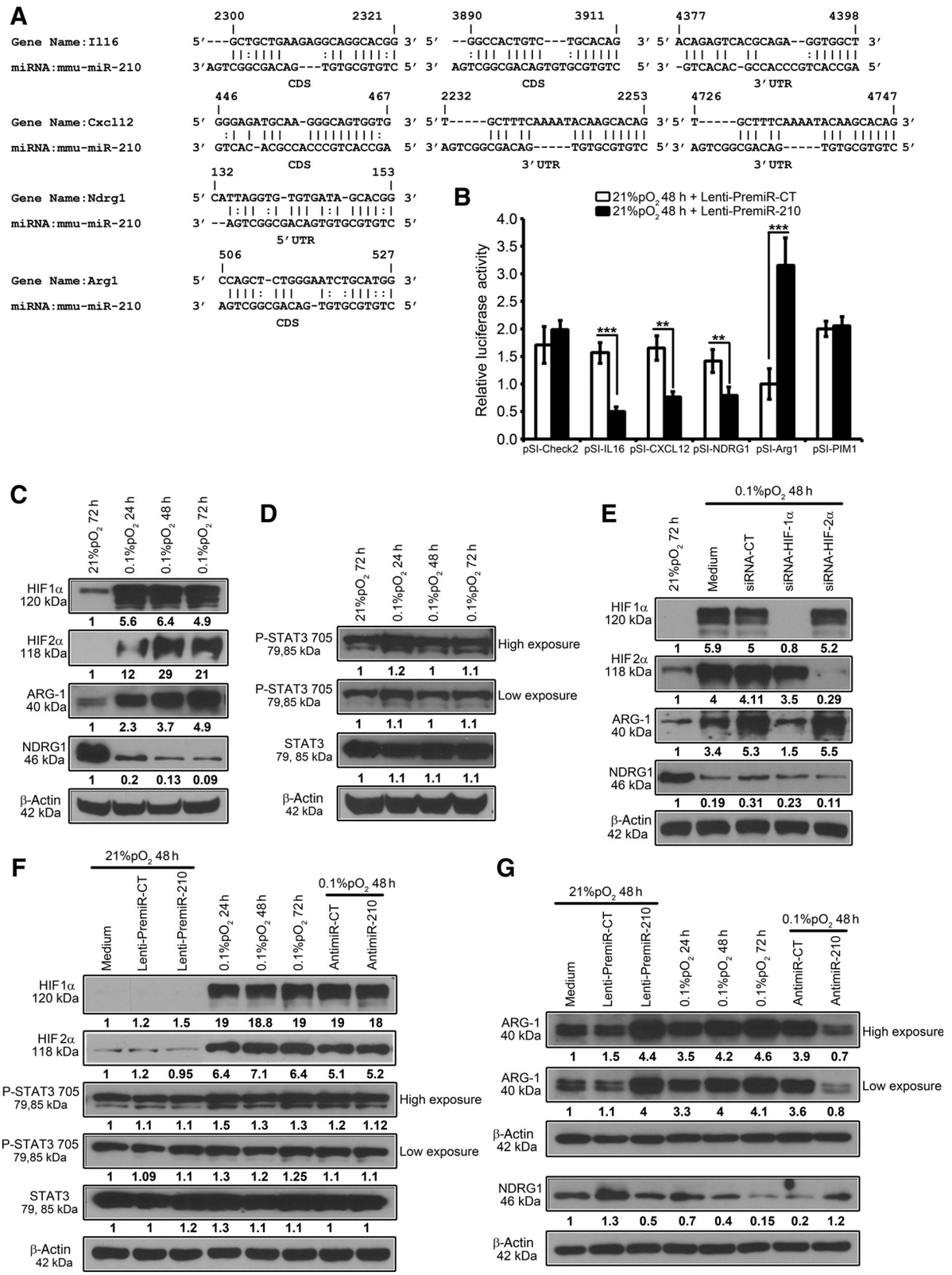

Published OnlineFirst July 23, 2015; DOI: 10.1158/0008-5472.CAN-15-0405

(under hypoxia) on either cytokines (IL6, IL10, IL12p70, and TGF-B1; Supplementary Fig. S2B) or immune checkpoint (PDL1, PDL2, PD1, and CTLA-4; Supplementary Fig. S2C) protein levels in B16-F10 MDSCs. We concluded that hypoxia-induced miR-210 modulates MDSCs function by increasing arginase activity and NO production and had no effect on ROS or their cytokine (IL6 and IL10) production and did not alter their PD-L1 expression.

miR-210 increases Arg1 expression and targets IL16 and CXCL12 in splenic MDSC

In order to identify the miR-210 potential target genes responsible for increased MDSCs function under hypoxia, we performed a comprehensive transcriptome analysis.

Using miRNA target predictions tool RNA22 version 1.0 (https://cm.jefferson.edu/rna22v1.0-mus_musculus/GetInputs.jsp), we selected a panel of 50 genes (predicted as mmu-miR-210 targets) among a list of more than 2,000 transcripts predicted to be targeted by mmu-miR-210. As shown in Supplementary Table S1, these genes were selected on the basis of their involvement in MDSCs proliferation, differentiation, and function. We further selected nine genes that meet the following criteria:

(1) Significantly downregulated or upregulated under hypoxia as compared with normoxia.
(2) Significantly upregulated or downregulated when hypoxic MSC-1 cells were transfected with anti-miR-210 as compared with anti-miR-CT.
(3) Significantly downregulated or upregulated when normoxic MSC-1 cells were transfected with PremiR-210 as compared with PremiR-CT (Supplementary Table S1).

Strikingly, overexpression of miR-210 under normoxia significantly increased the mRNA expression levels of Arg1, but not of Nos2 (Fig. 4A), and targeting miR-210 under hypoxia significantly decreased expression levels of Arg1, but not of Nos2 (Fig. 4B), in both B16-F10 splenic MDSCs and 4T1 splenic MDSCs. Similarly, miR-210 overexpression under normoxia decreased the mRNA expression levels of Acvr1b, Cxcl12, Il16, Ndrg1, Nptx1, Tcf7I2, and Ucp2 (Fig. 4A) and targeting miR-210 under hypoxia increased their expression levels (Fig. 4B) in both B16-F10 splenic MDSCs and 4T1 splenic MDSCs.

We next selected four genes (Arg1, Cxcl12, Il16, and Ndrg1) based on their involvement in MDSCs function. We observed significantly higher protein levels of Arg1 and lower levels of IL16 and CXCL12 in both B16-F10 splenic MDSCs (Fig. 4C) and 4T1 splenic MDSCs (Fig. 4D) under hypoxic conditions. As expected, we did not detect any effect of hypoxia on inducible nitric oxide synthase (iNOS) protein levels (Fig. 4C and D). Importantly, overexpression of miR-210 under normoxia significantly increased the protein levels of Arg1, but not of Nos2, while targeting miR-210 under hypoxia decreased expression levels of Arg1, but not of Nos2, in both B16-F10 splenic MDSCs (Fig. 4E) and 4T1 splenic MDSCs (Fig. 4F). A miR-210 overexpression under normoxia decreased the production of IL16 and CXCL12 and targeting miR-210 under hypoxia increased their production in both B16-F10 splenic MDSCs (Fig. 4E) and 4T1 splenic MDSCs (Fig. 4F). These results were further confirmed by ELISA (Fig. 4G). Taken together, these data strongly point to the regulation of Arg1, Cxcl12, and Il16 at both mRNA and protein levels by miR-210 in splenic MDSCs.

Arg1, Il16, Cxcl12, and Ndrg1 are new validated miR-210 target genes

To further validate the identified miR-210 target genes (Il16, Cxcl12, Ndrg1, and Arg1), we searched for mmu-miR-210–binding sites, and their corresponding heteroduplexes, by using miRNA target predictions tool RNA22 version 1.0 (Fig. 5A). We inserted mmu-miR-210–binding sites sequence from the 3′-UTR, 5′-UTR, or CDS of Il16, Cxcl12, Ndrg1, and Arg1 genes into pSI-check2 vector (Fig. 5A) and performed luciferase reporter assays. Our data indicated that Lenti-PremiR-210 significantly increased the luciferase activities of Arg1reporter, while it induced a significant decrease in the luciferase activities of Cxcl12, Il16, and Ndrg1 reporters, as compared with Lenti-PremiR-CT in MSC-1 cells (Fig. 5B). In contrast, pSI-check2 (empty vector control) and PIM1 reporter luciferase activities were not repressed by Lenti-PremiR-210, confirming that Cxcl12, Il16, and Ndrg1 mmu-miR-210 target sites directly mediates repression of the luciferase activity through seed-specific binding. Regarding Arg1, miR-210 binds directly to seed-specific binding site and induces Arg1 gene expression (both mRNA and protein levels) under normoxia by an unknown mechanism. We concluded that Il16, Cxcl12, Ndrg1, and Arg1 are validated target genes of miR-210 in MSC-1 cells.

We next examined whether HIFs, HIF1α or HIF2α, are involved in the upregulation of ARG-1 under hypoxia. MSC-1 cells were cultured under normoxia or hypoxia. Figure 5C clearly shows that protein levels of HIF1α, HIF2α, and ARG-1 (more than 5-fold) was increased, whereas protein levels of NDRG1 were decreased under hypoxia. No effect was observed on protein levels of P-STAT3 (705) and total STAT3 under hypoxia in MSC-1 cells (Fig. 5D). To analyze the respective role of HIF1α and HIF2α in the hypoxic upregulation of ARG-1, MSC-1 cell line was transfected with siRNA targeting HIF1α, HIF2α, or scrambled control. Western blot analysis clearly showed siRNA-mediated

Figure 5.
Validation of Arg1, Il16, Cxcl12, and Ndrg1 as miR-210 target genes. A, schematic view of miR-210 complementary binding sites in the 3′-UTR, 5′-UTR, or CDS of Il16, Cxcl12, Ndrg1, and Arg1 genes. B, MSC-1 cells were cotransfected with 10 nmol/L Lenti-PremiR-CT or Lenti-PremiR-210 and different pSI-Check-2 constructs. After 48 hours, cells were harvested and luciferase activities analyzed. All *Renilla* luciferase activities were normalized to the firefly luciferase activity. pSI-IL16, pSI-CXCL12, pSI-NDRG1, pSI-Arg1, and pSI-PIM1 correspond to distinct fragments of IL16, CXCL12, NDRG1, ARG1, and PIM1 3′-UTR, 5′-UTR, or CDS containing miR-210 putative binding sites, respectively. pSI-check2 was used as an empty vector control. Statistically significant differences (indicated by asterisks) are shown (*, $P < 0.05$; **, $P < 0.005$; ***, $P < 0.0005$). The experiment was performed in triplicates and repeated two times with the same results. Error bars, SD. C and D, MSC-1 cells were cultured with or without exposure to 0.1% pO_2 hypoxia at indicated times. Western blot analysis was performed to show HIF1α, HIF2α, ARG-1, NDRG1 (C), and P-STAT3 705, STAT3 (D) protein levels. E, MSC-1 cells were transfected with different siRNA, targeting HIF1α, HIF2α or scrambled control (CT), and cultured under hypoxia for 48 hours. Western blot analysis was performed to show HIF1α, HIF2α, ARG-1, and NDRG1 protein levels. F and G, MSC-1 cells, transfected with Lenti-PremiR-control (CT) or Lenti-PremiR-210 (under normoxia) and anti-miR-control (CT) or anti-miR-210 (under hypoxia), were cultured for 48 hours. Western blot analysis was performed to show HIF1α, HIF2α, P-STAT3 705, STAT3 (F), ARG-1, and NDRG1 (G) protein levels. β-Actin was used as a control. The experiment was repeated three times with the same results.

Published OnlineFirst July 23, 2015; DOI: 10.1158/0008-5472.CAN-15-0405

knockdown of HIF1α, but not HIF2α, under hypoxia decreased hypoxia upregulated ARG-1 in MSC-1 cells (Fig. 5E).

To assess whether miR-210 can regulate hypoxia-induced transcription factors (HIF1α, HIF2α, P-STAT3 705), MSC-1 cells were transfected with Lenti-PremiR-control (CT) or Lenti-PremiR-210 (under normoxia), and anti-miR-control (CT) or anti-miR-210 (under hypoxia), and then cultured for 48 hours. The Western blot analysis in Fig. 5F clearly shows that no effect was observed of miR-210 overexpression under normoxia, or when targeting miR-210 under hypoxia on HIF1α, HIF2α, P-STAT3 705, and total STAT3 protein levels in MSC-1 cells. However, overexpression of miR-210 under normoxia increased ARG-1 and decreased NDRG1 protein levels while targeting miR-210 under hypoxia decreased ARG-1 and increased NDRG1 protein levels in MSC-1 cells (Fig. 5G).

Targeting of Arg1 and blockade of IL16 and CXCL12 decreases MDSC function

We next asked whether miR-210 enhanced MDSCs function through its target genes (Arg1, Il16, Cxcl12, and Ndrg1). For this purpose, MDSCs, isolated from spleens of B16-F10 and 4T1 tumor-bearing mice, were transfected with siRNA targeting Ndrg1, Arg1, or scrambled control (CT) and cultured under normoxia and hypoxia for 48 hours. We found that a siRNA-mediated knockdown of Arg1, but not of Ndrg1 (both under normoxia and hypoxia), significantly decreased arginase activity in B16-F10 splenic MDSCs and 4T1 splenic MDSCs (Fig. 6A). Neutralizing antibodies against IL16 and CXCL12 under normoxia significantly abrogated the suppressive activity of both B16-F10 splenic MDSCs and 4T1 splenic MDSCs in response to anti-CD3/CD28 stimulation (Fig. 6B). Similarly, the ability of MDSC to inhibit T-cell function under normoxia decreased with both IL16 and CXCL12 neutralizing antibodies. The percentage of $IFN\gamma^+$ $CD8^+$ T cells and $IFN\gamma^+$ $CD4^+$ T cells decreased with both IL16 and CXCL12 blocking antibodies when splenocytes were cocultured with B16-F10 splenic MDSCs (Fig. 6C) and 4T1 splenic MDSCs (Fig. 6D).

Finally, neutralizing antibodies against IL16, but not CXCL12, under normoxia significantly decreased MDSCs ability to inhibit T-cell activation marker CD25. The percentage of $CD25^+$ $CD8^+$ T cells and $CD25^+$ $CD4^+$ T cells decreased with IL16, but not with CXCL12 blocking antibodies, when splenocytes were cocultured with B16-F10 splenic MDSCs (Fig. 6E) and 4T1 splenic MDSCs (6F). Altogether, our data indicate that miR-210 modulates MDSCs function through its regulation of Arg1, Il16, and Cxcl12.

miR-210 overexpression and IL16 or CXCL12 targeting alleviates the T cell–mediated immune suppression by MDSC in 4T1 tumor-bearing mice

Adoptive transfer of either splenic MDSCs from tumor-bearing mice or tumor-associated MDSCs have been reported to promote tumor growth (10). We hypothesized that miR-210 overexpressing MDSCs with enhanced immunosuppressive activity would promote tumor growth. Conversely, miR-210 knocked down MDSCs with decreased immunosuppressive activity would result in more potent antitumor effect.

MDSCs ($CD11b^+Gr1^+$ cells isolated from spleens of 4T1 tumor-bearing mice) were transfected with Lenti-PremiR-control (CT) or Lenti-PremiR-210 and anti-miR-control (CT) or anti-miR-210 and infused in 4T1 tumor-bearing Balb/c mice or 4T1 tumor-bearing nude mice (Fig. 7A). Interestingly, 4T1 tumor growth significantly increased in Balb/c mice infused with MDSCs transfected with Lenti-PremiR-210 as compared with Lenti-PremiR-CT (Fig. 7B and D). On the other hand, 4T1 tumor growth was found to be significantly slower in Balb/c mice infused with MDSCs transfected with anti-miR-210 as compared with anti-miR-CT (Fig. 7C and D). More importantly, miR-210 modulated MDSC-mediated immune suppression was totally dependent on T cells as no effect was observed on 4T1 tumor growth in nude mice. As shown in Fig. 7E and F, when MDSCs, transfected with either Lenti-PremiR-210 or anti-miR-210, were infused in nude mice, there was no difference in 4T1 tumor growth (Fig. 7G). These data clearly indicate that miR-210 affects *in vivo* MDSC-mediated T-cell suppression.

In these *in vivo* experiments (Fig. 7), controls like noninfused Balb/c mice or Balb/c mice infused with MDSCs without transfection were performed and gave similar results (4T1 tumor growth) as Balb/c mice infused with MDSCs transfected with Lenti-control (data not shown).

We next investigated whether miR-210 enhanced *in vivo* MDSCs function by increasing immune suppression and subsequent tumor growth through its target genes (IL16 and CXCL12). For this purpose, MDSCs ($CD11b^+Gr1^+$ cells isolated from spleens of 4T1 tumor-bearing mice) were transfected with Lenti-control (CT) and Lenti-IL16 or Lenti-CXCL12 and infused in 4T1 tumor-bearing Balb/c mice or 4T1 tumor-bearing nude mice (Fig. 7A). Interestingly, 4T1 tumor growth significantly increased in Balb/c mice infused with MDSCs transfected with either Lenti-IL16 or Lenti-CXCL12 as compared with Lenti-CT (Fig. 7H and I). More importantly, this IL16 and CXCL12 modulated MDSC-mediated immune suppression was totally dependent on T cells as no effect was observed on 4T1 tumor growth in nude mice (7J and K). Altogether, miR-210 via IL16 and CXCL12 affects MDSC-mediated T-cell suppression and *in vivo* tumor growth.

Discussion

It is widely accepted that the environment of a tumor is an integral part of its physiology, structure, and function. Its role during the initiation and progression of carcinogenesis is presently considered to be of critical importance, both for better understanding of fundamental tumor biology, and for exploiting this source of relatively new knowledge to improve molecular diagnostics and therapeutics. In this regard, hypoxia, a hallmark of most solid tumors, is a key determinant of tumor microenvironment (1). Recently, we showed that hypoxia selectively upregulated PD-L1, via HIF1α, by binding directly to the HRE in the PD-L1 proximal promoter and blockade of PD-L1 under hypoxia abrogated MDSC function by modulating MDSCs cytokine production (17). In addition, hypoxia, via HIFs, is capable of inducing a group of HIM, which, in turn, regulates several target genes, thereby fine tuning hypoxic response (1, 18). In this study, we attempted to identify HIM in MDSCs under hypoxia and investigate their prospective role in the regulation of MDSC immunosuppressive function.

We first showed that tumor-infiltrating MDSCs express increased levels of miR-210 and hypoxia markers (CA-IX and GLUT-1) as compared with splenic MDSCs. We also found that among the putative HIM, miR-210 was highly and significantly induced under hypoxia via HIF1α in splenic MDSC. Hypoxia selectively induced both mmu-miR-210-3p and mmu-

Published OnlineFirst July 23, 2015; DOI: 10.1158/0008-5472.CAN-15-0405

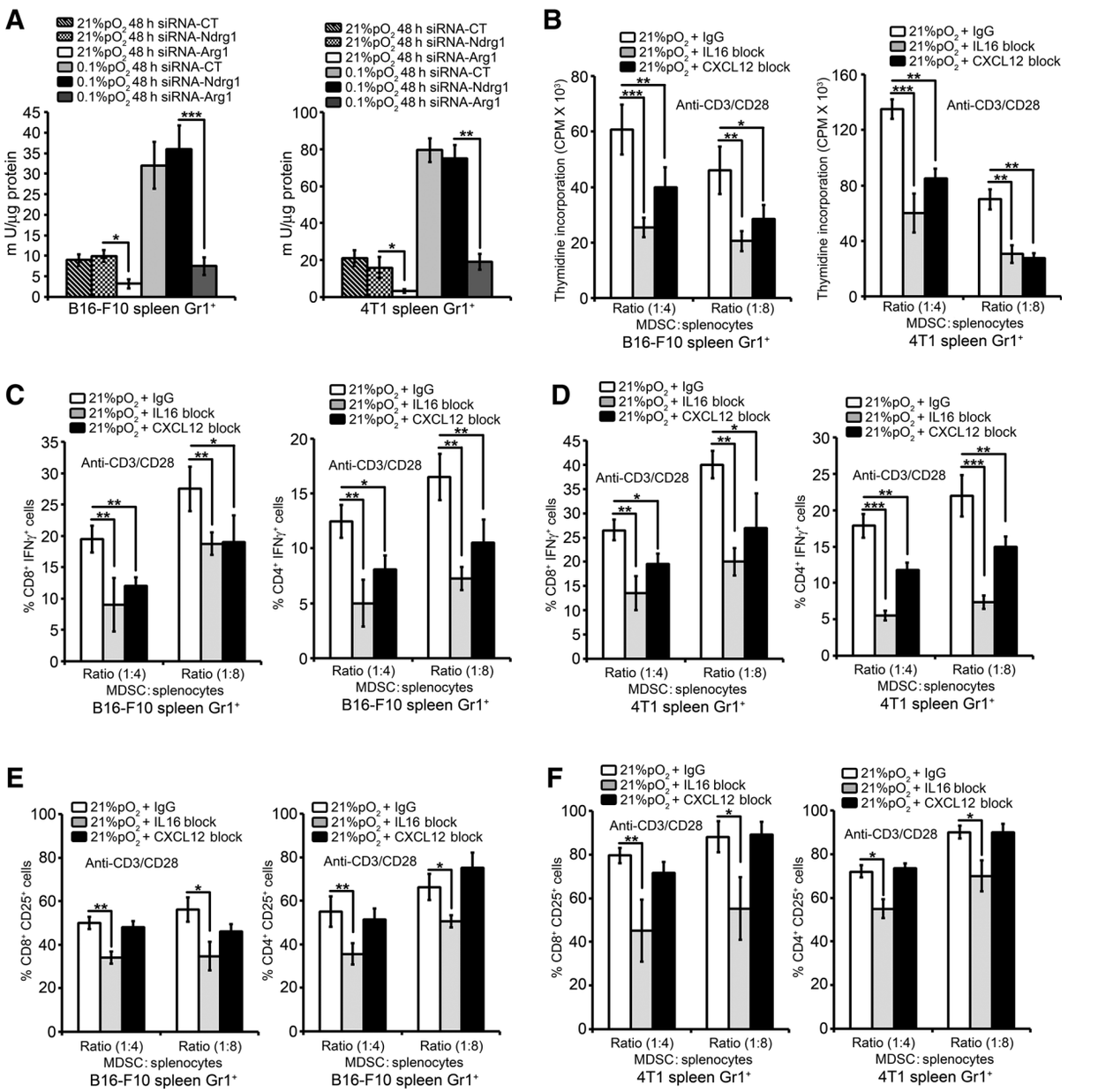

Figure 6.

miR-210 targets Arg1, Il16, and Cxcl12 modulate MDSC immunosuppressive function. A, MDSCs isolated from spleens of B16-F10 and 4T1 tumor-bearing mice were transfected with different siRNA, targeting Ndrg1, Arg1,or scrambled control (CT) and cultured under normoxia and hypoxia for 48 hours. Arginase enzymatic activity was measured in both B16-F10 spleen Gr1$^+$ MDSC and 4T1 spleen Gr1$^+$ MDSC cells under indicated conditions. Statistically significant differences (indicated by asterisks) are shown (*, $P < 0.05$; **, $P < 0.005$; ***, $P < 0.0005$). The experiment was performed in triplicates and repeated twice with the same results. Error bars, SD. B–F, MDSCs isolated from spleens of B16-F10 and 4T1 tumor-bearing mice were cocultured with splenocytes under normoxia for 72 hours in the presence of either 10 μg/mL control antibody (IgG), anti-mouse IL16 functional grade purified neutralizing antibody (IL16 Block), or anti-mouse CXCL12 functional grade purified neutralizing antibody (CXCL12 Block). Effect of B16-F10 spleen Gr1$^+$ MDSC and 4T1 spleen Gr1$^+$ MDSC (B) cells on proliferation of splenocytes was stimulated with anti-CD3/CD28-coated beads under the indicated conditions. Cell proliferation was measured in triplicates by thymidine (^{3}H) incorporation and expressed as CPM. C–F, B16-F10 spleen Gr1$^+$ MDSC (C and E) and 4T1 spleen Gr1$^+$ MDSC (D and F) cells were cultured with splenocytes stimulated with anti-CD3/CD28. C and D, intracellular IFNγ production was evaluated by flow cytometry by gating on CD3$^+$CD8$^+$ IFNγ$^+$ and CD3$^+$CD4$^+$ IFNγ$^+$ populations. E and F, T-cell activation marker CD25 was evaluated by flow cytometry by gating on CD3$^+$CD8$^+$ CD25$^+$ and CD3$^+$CD4$^+$ CD25$^+$ populations. Statistically significant differences (indicated by asterisks) are shown (*, $P < 0.05$; **, $P < 0.005$; ***, $P < 0.0005$). Two separate experiments (in triplicates) with the same results were performed. Error bars, SD.

miR-210-5p, but mmu-miR-210-3p was the most highly induced miR-210. In a large number of cancers, several HIM are induced in response to hypoxia, including miR-67, miR-21, and the miR-Let7 family (18), we did not observe any effect on their expression under hypoxia in MDSC. It should be noted that although several miRNAs, including miR-155 (12, 16), miR-494 (15), miR-223

Published OnlineFirst July 23, 2015; DOI: 10.1158/0008-5472.CAN-15-0405

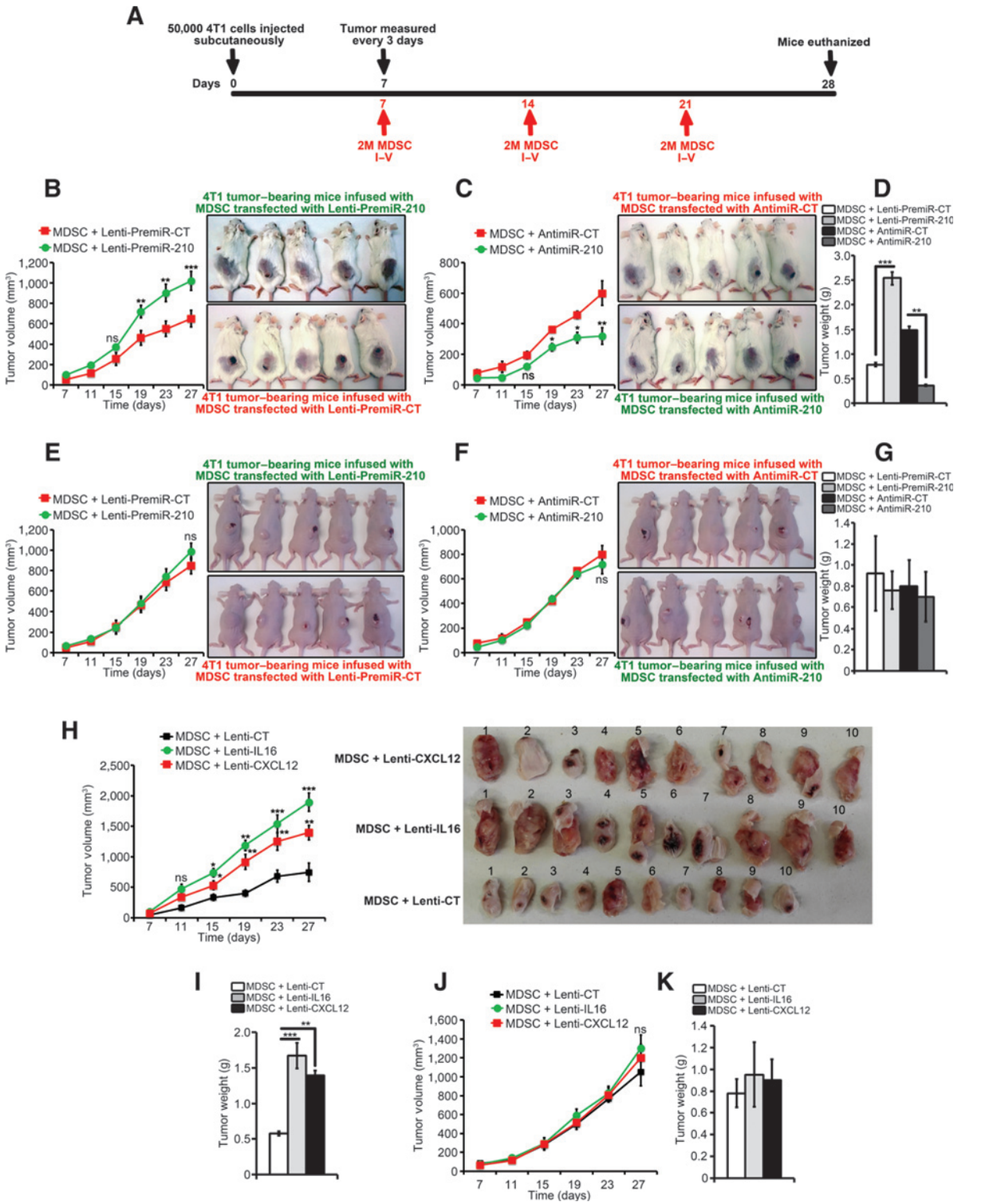

Figure 7.

Overexpression of miR-210 and IL16 or CXCL12 targeting alleviates the T cell–mediated immune suppression by MDSC in 4T1 tumor bearing mice. A–D, MDSCs ($CD11b^{+}Gr1^{+}$) cells were isolated from spleens of 4T1 tumor-bearing mice. MDSC were transfected with Lenti-PremiR-control (CT) or Lenti-PremiR-210 and anti-miR-control (CT) or anti-miR-210, and infused in 4T1 tumor-bearing Balb/c mice according to the protocol (A) described in Materials and Methods. Overexpression of miR-210 aggravate/alleviate MDSC function (B) while knocking down miR-210 decrease MDSC suppression (C). 4T1 Tumors were measured with a caliper and weighed by weighing scales (D). Statistically significant differences (indicated by asterisks) are shown (*, $P < 0.05$; **, $P < 0.005$; ***, $P < 0.0005$). Two separate experiments (5 mice per group) were performed. Error bars, mean SE. (*Continued on the following page.*)

Published OnlineFirst July 23, 2015; DOI: 10.1158/0008-5472.CAN-15-0405

(23), miR-17-5p, and miR-20a (14), were reported to be required for MDSC differentiation and function, hypoxia had only a slight or no effect on the expression of these miRNAs in MDSC.

miR-210, induced under hypoxia in various cell types, has been frequently reported as the master regulator of hypoxic tumor response in various cancers (18, 25). It participates in the hypoxic response of endothelial cells (26) and fibroblasts (27). More importantly, in human Tregs, miR-210 negatively regulated FOXP3 expression (28). Similarly, LPS-induced miR-210 negatively regulated murine macrophage production of proinflammatory cytokines by targeting NF-κB1 (29). Very recently, miR-210 was found to be robustly increased in activated T cells and negatively regulated Hif1a expression and TH17 differentiation (30). Here, we provide evidence for a selective induction of miR-210 via HIF1α in splenic MDSCs from tumor-bearing mice. The cellular distribution of hypoxia-induced miR-210 in major cellular populations present in the tumor microenvironment is not yet established. Whether miR-210 plays a differential role in tumors versus MDSC or macrophages or dendritic cells or T lymphocytes remains unexplored.

We and others have previously shown that hypoxia modulates MDSCs function (8, 17). In this study, we demonstrated that hypoxia-induced miR-210 regulated MDSC function. Our data strongly indicates that hypoxia-induced miR-210 is partly involved in mediating the suppressive MDSC activity, because we were not able to completely restore T-cell proliferation and function after miR-210 targeting on MDSCs under hypoxia. Thus, apart from hypoxia-induced HIF1α (8) and hypoxia upregulated PD-L1 (17), miR-210 is yet another novel critical modulator of MDSC function under hypoxic stress. It is well known that IL6, GM-CSF, or TGFβ promoted the induction of MDSC from the bone marrow cells through upregulation of miR-155 and miR-21 expression (also hypoxia-regulated miRNAs; ref. 22). It would be interesting to study whether cytokine (IL6, GM-CSF, or TGF-β)–mediated induction of MDSC from bone marrow cells will influence miR-210 expression.

It is important to note that miR-210 had no effect on IL6, IL10, and PD-L1 mRNA and protein levels. miR-210 modulated MDSCs function by regulating arginase activity and NO production but had no effect on ROS production. The role of HIFs and miR-210 in the modulation of hypoxia-induced ROS remains controversial. Conflicting studies have reported opposing effects of miR-210 on ROS generation under hypoxia (31, 32). These differences, appearing between different studies, seem to be dependent upon specific molecular context and the different methods of ROS detection. The observed decrease in ROS production in MDSC seems to be dependent upon HIF1α rather than miR-210 under hypoxia. This can be explained by the fact that miR-210 had no effect on ROS genes (cybb1 and Ncf1) in MDSC (Supplementary Table S1). Whether other HIM are responsible for hypoxic decrease in ROS levels remains to be established.

We demonstrated that miR-210 modulated Arg1expression but not of Nos2. Although both HIFs and miR-210 are induced under hypoxia, their simultaneous activation but antagonistic function may be important for hypoxic Arg1, NO, and ROS homeostasis in MDSCs. This would explain why hypoxia modulates Arg1, NO, and ROS production while only Arg1, but not NO and ROS genes, are regulated by miR-210. Such an association has been previously shown between different HIFs isoforms. In macrophages, differential activation and antagonistic function of HIF1α mRNA by Th1 cytokines, and HIF2α mRNA by Th2 cytokines, in M1- and M2-polarized macrophages, respectively, are essential for NO homeostasis by differential action on their two target genes: iNOS and arginase1 (33).

STAT1, STAT3, and STAT6 have been extensively reported to directly regulate the MDSCs immunosuppressive function (10). Recently, in head and neck squamous cell carcinoma patients, MDSCs expressed high phosphorylated STAT3 levels that binds directly to ARG1 promoter and regulate MDSC function by modulating ARG-1 expression levels and activity (34). Under normoxia, miR-17-5p and miR-20a have been shown to decrease MDSCs immunosuppressive potential by modulating STAT3 expression (14). Our results show that MDSCs have constitutively activated high levels of P-STAT3 under normoxia. Hypoxia induced a slight increase in both P-STAT3 and STAT3 protein levels, while miR-210 overexpression under normoxia, or its targeting under hypoxia, did not modulate P-STAT3 or STAT3 protein levels. We have previously reported that targeting STAT3, or inhibition of P-STAT3 under hypoxia, resulted in a complete inhibition of hypoxia-induced HIF1αin lung cancer (35). Whether HIFs, HIF1α or HIF2α, can modulate constitutively active P-STAT3 or STAT3 protein levels under hypoxia in MDSCs remains uninvestigated.

Hypoxia-induced miR-155 directly targets Hif1a in intestinal epithelial cells during prolonged hypoxia thereby completely inhibiting HIF1 transcriptional activity (36). Similarly, miR-210 was found to be increased in activated T cells and miR-210 negatively regulated Hif1a expression andTH17 differentiation (30). This seems to be specific for activated T cells as we did not observe any effect of miR-210 on HIF1α or HIF2α protein levels in MDSC under hypoxia or normoxia. Moreover, miR-155 was not regulated by hypoxia in splenic MDSCs.

Hypoxia-upregulated Arg-1 was found to be dependent upon HIF1α and overexpression of miR-210 under normoxia increased Arg-1 mRNA and protein levels. Targeting miR-210 under hypoxia decreased Arg-1 mRNA and protein levels in splenic MDSCs. Our results are in complete agreement with previous reports,

(*Continued.*) E–G, MDSCs ($CD11b^+Gr1^+$) cells were isolated from spleens of 4T1 tumor-bearing mice. MDSCs were transfected with Lenti-PremiR-control (CT) or Lenti-PremiR-210, and anti-miR-control (CT) or anti-miR-210, and infused in 4T1 tumor-bearing nude mice according to the protocol described in Materials and Methods. Overexpression of miR-210 (E) and knocking down miR-210 (F) had no effect on 4T1 tumor growth. 4T1 Tumors were measured with a caliper and weighed by weighing scales (G). Statistically significant differences (indicated by asterisks) are shown (*, $P < 0.05$; **, $P < 0.005$; ***, $P < 0.0005$). Two separate experiments (5 mice per group) were performed. Error bars, mean SE. H and I, MDSC ($CD11b^+Gr1^+$) cells were isolated from spleens of 4T1 tumor-bearing mice. MDSCs were transfected with either Lenti-control (CT) or Lenti-IL16 or Lenti-CXCL12 and infused in 4T1 tumor-bearing Balb/c mice according to the protocol described in A. 4T1 Tumors were measured with a caliper and weighed by weighing scales (I). Statistically significant differences (indicated by asterisks) are shown (*, $P < 0.05$; **, $P < 0.005$; ***, $P < 0.0005$). Two separate experiments (10 mice per group) were performed. Error bars, mean SE. J and K, MDSCs ($CD11b^+Gr1^+$) cells were isolated from spleens of 4T1 tumor-bearing mice. MDSC were transfected with either Lenti-control (CT) or Lenti-IL16 or Lenti-CXCL12 and infused in 4T1 tumor-bearing nude mice according to the protocol described in A. 4T1 Tumors were measured with a caliper and weighed by weighing scales (K). Statistically significant differences (indicated by asterisks) are shown (*, $P < 0.05$; **, $P < 0.005$; ***, $P < 0.0005$). Two separate experiments (10 mice per group) were performed. Error bars, mean SE.

Published OnlineFirst July 23, 2015; DOI: 10.1158/0008-5472.CAN-15-0405

indicating that HIF1α is able to mediate hypoxic regulation of Arg-1 in macrophages and MDSCs (8, 33).

More interestingly, miR-210 binds directly to seed-specific binding sites in promoter regions of Cxcl12, Il16, Ndrg1, and especially Arg1 and modulate their expression levels. miRNA commonly negatively regulates gene expression by repressing translation or directing sequence-specific degradation of complementary mRNA. Strikingly, miRNAs can switch from repression to activation, and miR-Let7 (37), miR-10a (38), and miR-373 (39) were reported to induce gene expression by upregulating translation. Similarly, miR-95, which is highly expressed in adult peripheral blood Tregs, was found to positively regulate FOXP3 expression via an unidentified, indirect mechanism (28). We found that miR-210 binds directly to seed-specific binding sites in promoter region and induces Arg1 gene expression (both mRNA and protein levels) under normoxia by an unknown mechanism. Future experiments will attempt to dissect whether miR-210 induces Arg1 gene expression by upregulating its translation, or by inhibiting its mRNA degradation.

We next found that miR-210 enhanced MDSC-mediated T-cell suppression through its target genes: Arg1, Il16, and Cxcl12 but not Ndrg1. Hypoxia via miR-210 decreased IL16 and CXCL12 secretion from MDSC, thereby inhibiting T-cell function. Our results are consistent with previous findings as CXCL12 was shown to be a costimulator for $CD4^+$ T-cell activation (40). Similarly, IL16 also regulates T-cell activation, IL2 production, antigen-induced upregulation of CD95 expression, and most importantly their CD25 expression (41). A similar role for IL16 was observed as neutralizing antibodies against IL16 under normoxia decreased MDSC's ability to inhibit T-cell activation marker CD25.

The promise of targeting miRNAs in cancer has now become a reality and therapeutic benefit of miRNA targeting are now achieved by either antagonizing or restoring miRNA function (42). Very interestingly, miR-210 overexpressing MDSCs and IL16- or CXCL12-silenced MDSCs enhanced immunosuppressive activity and promoted 4T1 tumor growth. Conversely, miR-210 knocked down MDSCs decreased immunosuppressive activity and resulted in a more potent antitumor effect. More importantly, this miR-210 modified MDSC-mediated immune suppression was totally dependent on T cells as no effect was observed on 4T1 tumor growth in nude mice. Similarly, miR-17-5p and miR-20a based miRNA targeting was found to decrease MDSC function through *in vivo* modulation of STAT3 expression (14).

Taken together, hypoxia selectively upregulated miR-210, via HIF1α in splenic MDSC, which modulated MDSCs function by increasing arginase activity and NO production. miR-210 regulated Arg1, Il16, and Cxcl12 at both mRNA and protein levels in splenic MDSCs. Overexpression or targeting of miR-210 affected MDSC-mediated T-cell suppression *in vivo*. These results establish a new link between miR-210 and MDSC-mediated immune suppression under hypoxia in the tumor microenvironment.

Hypoxia and HIF targeting has been suggested as a potential therapeutic target in cancer (1, 17). Therefore, the use of miR-210 inhibitor oligonucleotide as adjuvant tool with new emerging immunotherapeutic strategies may be beneficial for boosting the immune system in cancer patients.

Disclosure of Potential Conflicts of Interest

F. Martelli is a consultant/advisory board member for Gruppo Ospedaliero San Donato Foundation. No potential conflicts of interest were disclosed by the authors.

Authors' Contributions

Conception and design: M.Z. Noman, B. Janji, S. Chouaib
Development of methodology: M.Z. Noman, B. Janji, J.C. Wu, V. Bronte, S. Chouaib
Acquisition of data (provided animals, acquired and managed patients, provided facilities, etc.): M.Z. Noman, S. Hu, F. Martelli
Analysis and interpretation of data (e.g., statistical analysis, biostatistics, computational analysis): M.Z. Noman, S. Chouaib
Writing, review, and/or revision of the manuscript: M.Z. Noman, J.C. Wu, S. Chouaib
Administrative, technical, or material support (i.e., reporting or organizing data, constructing databases): M.Z. Noman, S. Chouaib
Study supervision: M.Z. Noman, S. Chouaib

Grant Support

This work was supported by a grant "Equipe labellisée Ligue Contre le Cancer," and B. Janji was supported by a grant from CRP-Santé (LHCE-2013-1105). F. Martelli was supported by Italian Ministry of Health and by Cariplo Foundation grant no. 2013-0887.

The costs of publication of this article were defrayed in part by the payment of page charges. This article must therefore be hereby marked *advertisement* in accordance with 18 U.S.C. Section 1734 solely to indicate this fact.

Received February 13, 2015; revised June 16, 2015; accepted June 26, 2015; published OnlineFirst July 23, 2015.

References

1. Noman MZ, Messai Y, Carre T, Akalay I, Meron M, Janji B, et al. Microenvironmental hypoxia orchestrating the cell stroma cross talk, tumor progression and antitumor response. Crit Rev Immunol 2011;31:357–77.
2. Semenza GL. Oxygen sensing, homeostasis, and disease. N Engl J Med 2011;365:537–47.
3. Palazon A, Aragones J, Morales-Kastresana A, de Landazuri MO, Melero I. Molecular pathways: hypoxia response in immune cells fighting or promoting cancer. Clin Cancer Res 2012;18:1207–13.
4. Cramer T, Yamanishi Y, Clausen BE, Forster I, Pawlinski R, Mackman N, et al. HIF-1alpha is essential for myeloid cell-mediated inflammation. Cell 2003;112:645–57.
5. Doedens AL, Stockmann C, Rubinstein MP, Liao D, Zhang N, DeNardo DG, et al. Macrophage expression of hypoxia-inducible factor-1 alpha suppresses T-cell function and promotes tumor progression. Cancer Res 2010;70:7465–75.
6. Facciabene A, Peng X, Hagemann IS, Balint K, Barchetti A, Wang LP, et al. Tumour hypoxia promotes tolerance and angiogenesis via CCL28 and T (reg) cells. Nature 2011;475:226–30.
7. Clambey ET, McNamee EN, Westrich JA, Glover LE, Campbell EL, Jedlicka P, et al. Hypoxia-inducible factor-1 alpha-dependent induction of FoxP3 drives regulatory T-cell abundance and function during inflammatory hypoxia of the mucosa. Proc Natl Acad Sci U S A 2012;109:E2784–93.
8. Corzo CA, Condamine T, Lu L, Cotter MJ, Youn JI, Cheng P, et al. HIF-1alpha regulates function and differentiation of myeloid-derived suppressor cells in the tumor microenvironment. J Exp Med 2010;207:2439–53.
9. Youn JI, Nagaraj S, Collazo M, Gabrilovich DI. Subsets of myeloid-derived suppressor cells in tumor-bearing mice. J Immunol 2008;181:5791–802.
10. Gabrilovich DI, Ostrand-Rosenberg S, Bronte V. Coordinated regulation of myeloid cells by tumours. Nat Rev Immunol 2012;12:253–68.
11. O'Connell RM, Rao DS, Chaudhuri AA, Baltimore D. Physiological and pathological roles for microRNAs in the immune system. Nat Rev Immunol 2010;10:111–22.
12. O'Connell RM, Chaudhuri AA, Rao DS, Baltimore D. Inositol phosphatase SHIP1 is a primary target of miR-155. Proc Natl Acad Sci U S A 2009;106:7113–8.

13. Sonda N, Simonato F, Peranzoni E, Cali B, Bortoluzzi S, Bisognin A, et al. miR-142–3p prevents macrophage differentiation during cancer-induced myelopoiesis. Immunity 2013;38:1236–49.
14. Zhang M, Liu Q, Mi S, Liang X, Zhang Z, Su X, et al. Both miR-17–5p and miR-20a alleviate suppressive potential of myeloid-derived suppressor cells by modulating STAT3 expression. J Immunol 2011;186:4716–24.
15. Liu Y, Lai L, Chen Q, Song Y, Xu S, Ma F, et al. MicroRNA-494 is required for the accumulation and functions of tumor-expanded myeloid-derived suppressor cells via targeting of PTEN. J Immunol 2012;188:5500–10.
16. Wang J, Yu F, Jia X, Iwanowycz S, Wang Y, Huang S, et al. microRNA-155 deficiency enhances the recruitment and functions of myeloid-derived suppressor cells in tumor microenvironment and promotes solid tumor growth. Int J Cancer 2015;136:E602–13.
17. Noman MZ, Desantis G, Janji B, Hasmim M, Karray S, Dessen P, et al. PD-L1 is a novel direct target of HIF-1alpha, and its blockade under hypoxia enhanced MDSC-mediated T cell activation. J Exp Med 2014;211:781–90.
18. Kulshreshtha R, Davuluri RV, Calin GA, Ivan M. A microRNA component of the hypoxic response. Cell Death Differ 2008;15:667–71.
19. Hu S, Huang M, Li Z, Jia F, Ghosh Z, Lijkwan MA, et al. MicroRNA-210 as a novel therapy for treatment of ischemic heart disease. Circulation 2010;122:S124–31.
20. Cicchillitti L, Di Stefano V, Isaia E, Crimaldi L, Fasanaro P, Ambrosino V, et al. Hypoxia-inducible factor 1-alpha induces miR-210 in normoxic differentiating myoblasts. J Biol Chem 2012;287:44761–71.
21. Porichis F, Hart MG, Griesbeck M, Everett HL, Hassan M, Baxter AE, et al. High-throughput detection of miRNAs and gene-specific mRNA at the single-cell level by flow cytometry. Nat Commun 2014;5:5641.
22. Li L, Zhang J, Diao W, Wang D, Wei Y, Zhang CY, et al. MicroRNA-155 and MicroRNA-21 promote the expansion of functional myeloid-derived suppressor cells. J Immunol 2014;192:1034–43.
23. Liu Q, Zhang M, Jiang X, Zhang Z, Dai L, Min S, et al. miR-223 suppresses differentiation of tumor-induced CD11b(+) Gr1(+) myeloid-derived suppressor cells from bone marrow cells. Int J Cancer 2011;129:2662–73.
24. Apolloni E, Bronte V, Mazzoni A, Serafini P, Cabrelle A, Segal DM, et al. Immortalized myeloid suppressor cells trigger apoptosis in antigen-activated T lymphocytes. J Immunol 2000;165:6723–30.
25. Noman MZ, Buart S, Romero P, Ketari S, Janji B, Mari B, et al. Hypoxia-inducible miR-210 regulates the susceptibility of tumor cells to lysis by cytotoxic T cells. Cancer Res 2012;72:4629–41.
26. Fasanaro P, D'Alessandra Y, Di Stefano V, Melchionna R, Romani S, Pompilio G, et al. MicroRNA-210 modulates endothelial cell response to hypoxia and inhibits the receptor tyrosine kinase ligand Ephrin-A3. J Biol Chem 2008;283:15878–83.
27. Bodempudi V, Hergert P, Smith K, Xia H, Herrera J, Peterson M, et al. miR-210 promotes IPF fibroblast proliferation in response to hypoxia. Am J Physiol Lung Cell Mol Physiol 2014;307:L283–94.
28. Fayyad-Kazan H, Rouas R, Fayyad-Kazan M, Badran R, El Zein N, Lewalle P, et al. MicroRNA profile of circulating CD4-positive regulatory T cells in human adults and impact of differentially expressed microRNAs on expression of two genes essential to their function. J Biol Chem 2012;287:9910–22.
29. Qi J, Qiao Y, Wang P, Li S, Zhao W, Gao C. microRNA-210 negatively regulates LPS-induced production of proinflammatory cytokines by targeting NF-kappaB1 in murine macrophages. FEBS letters 2012;586:1201–7.
30. Wang H, Flach H, Onizawa M, Wei L, McManus MT, Weiss A. Negative regulation of Hif1a expression and TH17 differentiation by the hypoxia-regulated microRNA miR-210. Nat Immunol 2014;15:393–401.
31. Chan SY, Zhang YY, Hemann C, Mahoney CE, Zweier JL, Loscalzo J. MicroRNA-210 controls mitochondrial metabolism during hypoxia by repressing the iron-sulfur cluster assembly proteins ISCU1/2. Cell Metab 2009;10:273–84.
32. Mutharasan RK, Nagpal V, Ichikawa Y, Ardehali H. microRNA-210 is upregulated in hypoxic cardiomyocytes through Akt- and p53-dependent pathways and exerts cytoprotective effects. Am J Physiol Heart Circ Physiol 2011;301:H1519–30.
33. Takeda N, O'Dea EL, Doedens A, Kim JW, Weidemann A, Stockmann C, et al. Differential activation and antagonistic function of HIF-{alpha} isoforms in macrophages are essential for NO homeostasis. Genes Dev 2010;24:491–501.
34. Vasquez-Dunddel D, Pan F, Zeng Q, Gorbounov M, Albesiano E, Fu J, et al. STAT3 regulates arginase-I in myeloid-derived suppressor cells from cancer patients. J Clin Invest 2013;123:1580–9.
35. Noman MZ, Buart S, Van Pelt J, Richon C, Hasmim M, Leleu N, et al. The cooperative induction of hypoxia-inducible factor-1 alpha and STAT3 during hypoxia induced an impairment of tumor susceptibility to CTL-mediated cell lysis. J Immunol 2009;182:3510–21.
36. Bruning U, Cerone L, Neufeld Z, Fitzpatrick SF, Cheong A, Scholz CC, et al. MicroRNA-155 promotes resolution of hypoxia-inducible factor 1alpha activity during prolonged hypoxia. Mol Cell Biol 2011;31:4087–96.
37. Vasudevan S, Tong Y, Steitz JA. Switching from repression to activation: microRNAs can up-regulate translation. Science 2007;318:1931–4.
38. Orom UA, Nielsen FC, Lund AH. MicroRNA-10a binds the 5′UTR of ribosomal protein mRNAs and enhances their translation. Mol Cell 2008;30:460–71.
39. Place RF, Li LC, Pookot D, Noonan EJ, Dahiya R. MicroRNA-373 induces expression of genes with complementary promoter sequences. Proc Natl Acad Sci U S A 2008;105:1608–13.
40. Nanki T, Lipsky PE. Cutting edge: stromal cell-derived factor-1 is a costimulator for $CD4^+$ T cell activation. J Immunol 2000;164:5010–4.
41. Cruikshank WW, Lim K, Theodore AC, Cook J, Fine G, Weller PF, et al. IL-16 inhibition of CD3-dependent lymphocyte activation and proliferation. J Immunol 1996;157:5240–8.
42. Garzon R, Marcucci G, Croce CM. Targeting microRNAs in cancer: rationale, strategies and challenges. Nat Rev Drug Discov 2010;9:775–89.

Published OnlineFirst July 23, 2015; DOI: 10.1158/0008-5472.CAN-15-0405

Cancer Research
The Journal of Cancer Research (1916–1930) | The American Journal of Cancer (1931–1940)

AACR American Association for Cancer Research

Tumor-Promoting Effects of Myeloid-Derived Suppressor Cells Are Potentiated by Hypoxia-Induced Expression of miR-210

Muhammad Zaeem Noman, Bassam Janji, Shijun Hu, et al.

Cancer Res 2015;75:3771-3787. Published OnlineFirst July 23, 2015.